

1 **Oligomerization-driven MLKL ubiquitylation antagonises necroptosis**

2

3 Zikou Liu<sup>1,2</sup>, Laura F. Dagley<sup>1,2</sup>, Kristy Shield-Artin<sup>1,2</sup>, Samuel N. Young<sup>1</sup>, Aleksandra  
4 Bankovacki<sup>1,6</sup>, Xiangyi Wang<sup>1,2</sup>, Michelle Tang<sup>3,4</sup>, Jason Howitt<sup>3,4</sup>, Che A. Stafford<sup>5</sup>, Ueli  
5 Nachbur<sup>1,2</sup>, Cheree Fitzgibbon<sup>1</sup>, Sarah E. Garnish<sup>1,2</sup>, Andrew I. Webb<sup>1,2</sup>, David Komander<sup>1,2</sup>,  
6 James M. Murphy<sup>1,2</sup>, Joanne M. Hildebrand<sup>1,2^</sup>, John Silke<sup>1,2^</sup>

7

8 <sup>1</sup>The Walter and Eliza Hall Institute of Medical Research, Parkville, VIC 3052, Australia

9 <sup>2</sup>Department of Medical Biology, University of Melbourne, Parkville, VIC 3052, Australia

10 <sup>3</sup>The Florey Institute of Neuroscience and Mental Health, Parkville, VIC 3052, Australia

11 <sup>4</sup>Swinburne University of Technology, Hawthorn, VIC 3122, Australia

12 <sup>5</sup>Gene Centre and Department of Biochemistry, Ludwig Maximilian University of Munich,  
13 Munich 80331, Germany

14 <sup>6</sup>Translational Research, CSL Limited, Melbourne, VIC 3010, Australia

15 ^ Corresponding authors

16

17 **Running Title**

18 MLKL ubiquitylation during necroptosis

19

## 1 **Abstract**

2 Mixed lineage kinase domain-like (MLKL) is the executioner in the caspase-independent  
3 form of programmed cell death called necroptosis. Receptor Interacting serine/threonine  
4 Protein Kinase 3 (RIPK3) phosphorylates MLKL, triggering MLKL oligomerization,  
5 membrane translocation and membrane disruption. MLKL also undergoes ubiquitylation  
6 during necroptosis, yet neither the mechanism nor significance of this event have been  
7 demonstrated. Here we show that necroptosis-specific, multi-mono-ubiquitylation of MLKL  
8 occurs following its activation and oligomerization. Ubiquitylated MLKL accumulates in a  
9 digitonin insoluble cell fraction comprising plasma/organellar membranes and protein  
10 aggregates. This ubiquitylated form is diminished by a plasma membrane located  
11 deubiquitylating enzyme. MLKL is ubiquitylated on at least 4 separate lysine residues once  
12 oligomerized, and this correlates with proteasome- and lysosome- dependent turnover. Using  
13 a MLKL-DUB fusion strategy, we show that constitutive removal of ubiquitin from MLKL  
14 licences MLKL auto-activity independent of necroptosis signalling in mouse and human cells.  
15 Therefore, besides its role in the kinetic regulation of MLKL-induced death following an  
16 exogenous necroptotic stimulus, ubiquitylation also contributes to the restraint of basal levels  
17 of activated MLKL to avoid errant cell death.

18

## 19 **Key words**

20 Membranes/MLKL/necroptosis/DUB-fusion/ubiquitylation

21

## 22 **Introduction**

23 Necroptosis is a type of programmed cell death that shares some molecular components with  
24 the better-known apoptotic cell death pathway, but has distinct morphological features and  
25 different physiological consequences. Unlike apoptosis, which is immunologically silent and  
26 can be rapidly cleared by neighbouring phagocytic cells (Segawa & Nagata, 2015),  
27 necroptosis induces an inflammatory response by releasing cellular contents including DNA  
28 and cytosolic proteins (Kaczmarek *et al*, 2013). Necroptosis can be induced by a number of  
29 stimuli, but is mainly studied downstream of Tumor Necrosis Factor (TNF) ligation to its  
30 receptor Tumor Necrosis Factor Receptor 1 (TNFR1). If Inhibitor of Apoptosis (IAP)  
31 proteins and caspase activities are suppressed, this results in higher order assemblies of  
32 Receptor Interacting serine/threonine Protein Kinase 1 (RIPK1) and RIPK3, and subsequent  
33 RIPK3 activation and auto-phosphorylation (Sun *et al*, 2002; Wu *et al*, 2014). MLKL is

1 phosphorylated by RIPK3 and oligomerizes, translocates to biological membranes and  
2 induces organelle and cell swelling and membrane rupture (Petrie *et al*, 2019a; Vanden  
3 Berghe *et al*, 2015).

4  
5 Ubiquitylation plays a pivotal role in regulating TNF signalling. In addition to RIPK1  
6 ubiquitylation by cIAPs, which forms a platform for MAPK and NF- $\kappa$ B activation (Bertrand  
7 *et al*, 2008), the Linear Ubiquitin Chain Assembly Complex (LUBAC), composed of HOIL-1,  
8 HOIP and SHARPIN, generates M1-linked ubiquitin chains on RIPK1, TRADD, TNFR1 and  
9 NEMO. This ubiquitylation leads to full activation of IKK and MAPK, and limits TNF  
10 induced cell death (Haas *et al*, 2009; Ikeda *et al*, 2011; Tokunaga *et al*, 2009). LUBAC also  
11 recruits CYLD, a deubiquitylating enzyme (DUB), that removes M1- and K63-linked  
12 ubiquitin chains on RIPK1 and other complex components, while A20 sterically protects M1-  
13 linked ubiquitin chains (Dondelinger *et al*, 2016; Draber *et al*, 2015).

14  
15 Ubiquitylation has been implicated in the regulation of signalling checkpoints during  
16 necroptosis. RIPK3 undergoes K63-linked ubiquitylation on Lys-5, which is believed to  
17 support the formation of necrosome. Removal of this ubiquitin chain by the ubiquitin-editing  
18 enzyme A20 was proposed to negate necroptosis, because A20 loss led to RIPK3-dependent  
19 necroptosis in T cells and fibroblasts (Onizawa *et al*, 2015). Furthermore, ubiquitylated  
20 TRAF2 was reported to be associated with inactive MLKL, and CYLD deubiquitylates  
21 TRAF2 following necroptotic stimulation, allowing TRAF2 to dissociate from MLKL and  
22 MLKL to engage with, and be activated by, RIPK3 (Petersen *et al*, 2015).

23  
24 MLKL has also been shown to undergo ubiquitylation upon necroptotic stimulation  
25 (Hildebrand *et al*, 2020; Lawlor *et al*, 2015), yet the significance of this post-translational  
26 modification and its signalling function are unknown. Here we show that necroptotic  
27 signalling stimulates MLKL ubiquitylation and that this antagonises necroptosis *via*  
28 restraining the protein level of activated MLKL. MLKL oligomerization is the crucial stage  
29 for MLKL ubiquitylation, but RIPK3 phosphorylation is not necessary because auto-active  
30 oligomerizable MLKL mutants are ubiquitylated. MLKL ubiquitylation was removed *in vitro*  
31 by USP21, but not by other chain specific deubiquitylating enzymes, suggesting that MLKL  
32 is mono-ubiquitylated at multiples sites. Upon necroptotic stimulation, MLKL variants that  
33 are unable to induce cell death can still be ubiquitylated and this correlates with

1 proteasome/lysosome mediated turnover. Conversely, mutation of four lysine residues  
2 identified by mass spectrometry analysis to be ubiquitylated following a necroptotic stimulus  
3 did not affect MLKL ubiquitylation or MLKL's cytotoxic activity. We therefore devised a  
4 novel approach to completely remove all ubiquitins from MLKL by fusing it to USP21. We  
5 showed that this MLKL-USP21 fusion was resistant to ubiquitylation in both human and  
6 mouse cell lines and was more cytotoxic when compared with MLKL fused to a catalytically-  
7 inactive USP21. Strikingly, human MLKL, which is very resistant to auto-activation (Petrie  
8 *et al*, 2018; Tanzer *et al*, 2016), was auto-activated by the USP21 fusion suggesting that  
9 ubiquitylation is a major break on the activation of human MLKL.

## 1 **Results**

2

### 3 **MLKL becomes ubiquitylated during necroptosis**

4 MLKL has previously been reported to undergo ubiquitylation in mouse bone marrow-  
5 derived macrophages (BMDMs) stimulated with the necroptotic stimulus: LPS/Smac-  
6 mimetic (Compound A)/pan-caspase inhibitor (Q-VD-OPh) (Lawlor *et al.*, 2015). To test  
7 whether MLKL ubiquitylation is specific to necroptosis, we stimulated wildtype mouse  
8 dermal fibroblasts (MDFs) with TNF (T), Smac-mimetic (S) and the pan-caspase inhibitor  
9 IDN-6556 (I) individually or in combination for 3 hrs. GST-UBA immobilised on glutathione  
10 sepharose beads (Hospenthal *et al.*, 2015; Stafford *et al.*, 2018) was used to purify  
11 ubiquitylated proteins from cell lysates. These purified samples generated a distinct ladder of  
12 between 50 and 75 kDa when probed with anti-MLKL, which corresponds to non-  
13 ubiquitylated MLKL, mono-ubiquitylated MLKL and multi-ubiquitylated MLKL (**Fig. 1A**).  
14 Ubiquitylated MLKL species were only clearly detected for stimuli that promote MLKL  
15 phosphorylation (TI and TSI), but not for stimuli that induce apoptotic cell death (TS) (**Fig.**  
16 **1A**). Ubiquitylation appears to occur in the same time window as membrane permeabilization,  
17 because by the time of UBA-pulldown (UBA-PD) for MDFs (3 hrs) and HT29 cells (16 hrs),  
18 cells were ~60% propidium iodide (PI)-positive (**Supp. Fig. 1A**).

19

20 As expected, TSI failed to induce MLKL ubiquitylation in *Tnfr1*<sup>-/-</sup> MDFs, but, interestingly,  
21 did not completely prevent all TSI induced MLKL phosphorylation (**Fig. 1B**). Furthermore,  
22 the kinase activities of RIPK1 and RIPK3 were required for MLKL ubiquitylation because  
23 genetic deletion of *Ripk3*, or treatment with the RIPK1 and RIPK3 inhibitors, Nec-1 and  
24 GSK872, respectively, prevented MLKL ubiquitylation (**Fig. 1B**). MLKL phosphorylation  
25 and ubiquitylation were not, however, reduced by genetic deletion of *Traf2* (**Fig. 1B**). To test  
26 whether MLKL ubiquitylation occurred in other cell types, we examined mouse BMDMs.  
27 Necroptosis can be induced in BMDMs by a range of different ligands including LPS, Poly  
28 I:C and the TNF- receptor superfamily ligand FasL, when they are combined with a Smac-  
29 mimetic and a caspase inhibitor, IDN-6556 (SI) (Holler *et al.*, 2000; Kaiser *et al.*, 2013). To  
30 exclude a role for autocrine TNF, whose synthesis can be induced by a Smac-mimetic, LPS,  
31 poly I:C or FasL, we compared BMDMs isolated from *Tnf*<sup>-/-</sup> and WT mice, and saw the same  
32 MLKL ubiquitin laddering pattern in both. This ubiquitylation correlated with MLKL  
33 phosphorylation on S345, a well-known hallmark of MLKL activation and necroptosis (**Fig.**

1 **1C)** (Murphy *et al.*, 2013). We and others have shown that human and mouse MLKL are  
2 regulated distinctly (Davies *et al.*, 2020; Davies *et al.*, 2018; Li *et al.*, 2015; Petrie *et al.*, 2018;  
3 Tanzer *et al.*, 2016), therefore to see whether human MLKL was also ubiquitylated during  
4 necroptosis, we treated the human colonic adenocarcinoma HT29 cell line with TSI.  
5 Although induction of necroptosis takes longer in HT29 than in MDFs (**Supp. Fig. 1B**), we  
6 observed similar MLKL phosphorylation and ubiquitylation in HT29 cells as in MDFs with  
7 similar levels of cell death (**Fig. 1D, Supp. Fig. 1B**).

8  
9 To determine to what extent upstream necroptotic signalling was required for MLKL  
10 ubiquitylation, we used a well-established RIPK3 dimerization strategy to activate RIPK3 in  
11 the absence of necroptotic signals (Moujalled *et al.*, 2014; Orozco *et al.*, 2014). We therefore  
12 stably expressed a doxycycline-inducible RIPK3-gyrase fusion protein, which can be  
13 dimerized and activated by coumermycin (Moujalled *et al.*, 2014), in *Ripk3*<sup>-/-</sup> MDFs. As  
14 expected, forced dimerization of RIPK3 induced MLKL phosphorylation but was also able to  
15 induce MLKL ubiquitylation independent of TSI stimulation and to similar levels as TSI,  
16 indicating that RIPK3 dimerization and activation is sufficient to induce MLKL  
17 ubiquitylation (**Fig. 1E**).

18

### 19 **MLKL is ubiquitylated on multiple sites during necroptosis**

20 Ubiquitin can be coupled to, predominantly, lysine residues in target proteins. Ubiquitin itself  
21 contains 8 ubiquitylation sites (M1, K6, K11, K27, K29, K33, K48 and K63), which leads to  
22 the formation of ubiquitin chains of varying architectures. Differently linked Ub chains serve  
23 distinct functions in cells (Swatek & Komander, 2016). To investigate the ubiquitin  
24 architecture on MLKL, we purified ubiquitylated proteins from necroptotic cells using  
25 sepharose beads coupled with GST-UBA and digested them on the beads with a set of  
26 linkage selective deubiquitylating enzymes (UbiCRest) (Hospenthal *et al.*, 2015). Each DUB  
27 specifically recognizes and removes a known subset of poly-ubiquitin chain type with  
28 validated activity (**Fig. 2A**) (Stafford *et al.*, 2018). The non-specific DUB USP21 (Ye *et al.*,  
29 2011) converted MLKL into a non-ubiquitylated form, but the other chain-specific DUBs  
30 made no discernible difference to the MLKL ubiquitin laddering pattern (**Fig. 2B**). To control  
31 that there was sufficient DUB activity we decreased the ratio of substrate to DUBs to 1/2 and  
32 1/4 (**Fig. 2C**). vOTU, a DUB that can cleave every type of poly-ubiquitin chain except M1-  
33 linked chains, deubiquitylated most ubiquitylated proteins (see total ubiquitin blot, **Fig. 2C**),

1 yet it only deubiquitylated the highest molecular weight species of MLKL~Ub adducts, and  
2 did not affect bands representing the lower molecular weight MLKL~Ub species. No changes  
3 were observed upon treatment with OTULIN, a DUB specific for M1-linked ubiquitin chains  
4 (Keusekotten *et al*, 2013), indicating that the residual Ub left by vOTU are not M1-linked  
5 ubiquitin chains. Given that USP21 is the only DUB in the tested panel that can cleave the  
6 covalent bond between a protein substrate and the first ubiquitin unit added, these data  
7 suggest that ubiquitylated MLKL is most likely mono-ubiquitylated at multiple sites.

8

9 **MLKL ubiquitylation accumulates in the membrane fraction and can be**  
10 **deubiquitylated by USP21 localised to the plasma membrane**

11 During necroptosis, activated MLKL oligomerizes and translocates to biological membranes,  
12 ultimately causing membrane rupture and cell death (Cai *et al*, 2014; Chen *et al*, 2014;  
13 Hildebrand *et al*, 2014). To understand more about MLKL ubiquitylation, we examined when  
14 and where this occurs. WT MDFs were stimulated with TSI over a time course from 30 to  
15 180 minutes. Cytosolic and crude membrane fractions were generated as previously  
16 described using digitonin (Liu *et al*, 2018), and subjected to UBA-pull down. We refer to the  
17 0.025% digitonin insoluble fraction as ‘crude membrane’, but do not exclude the potential for  
18 non-membrane associated large macromolecular/amyloid-like structures to sediment along  
19 with crude membranes (Liu *et al*, 2017). Ubiquitylated MLKL emerged and accumulated  
20 within the whole cell lysate and the crude membrane fraction from 90 minutes post-stimulus  
21 onwards, coinciding precisely with the appearance of phosphorylated MLKL and onset of  
22 cell death (**Fig. 3A & Supp. Fig. 1A**). On the other hand, the predominant species of MLKL  
23 in the cytosol was non-phosphorylated and non-ubiquitylated (**Fig. 3A**). These data suggest  
24 that MLKL ubiquitylation occurs in the crude membrane fraction but not in the cytosol.

25

26 To explore further where ubiquitylated MLKL is located we took advantage of the fact that  
27 ubiquitylated MLKL was digested by USP21 (**Fig. 2B**). We therefore fused a CaaX motif tag  
28 (C=cysteine, a=aliphatic amino acid, X=terminal residue) to the C-terminus of the catalytic  
29 domain USP21 to localise it to the plasma membrane (Hancock *et al*, 1991). We chose  
30 ‘CVLQ’ to mimic the CaaX motif found at the C-terminal end of another DUB, USP32  
31 (Sapmaz *et al*, 2019), and also generated a catalytically-dead USP21 mutant version  
32 (USP21<sup>C221R</sup>) as a control, also fused with CaaX motif. This mutant, like the previously  
33 published mutant USP21<sup>C221A</sup>, lacks the ability to remove ubiquitin (Morrow *et al*, 2018; Ye  
34 *et al.*, 2011; Ye *et al*, 2012). Using these stably and inducibly expressed constructs we

1 evaluated TSI-mediated MLKL ubiquitylation with or without USP21-CaaX function. Taking  
2 into account the amount of MLKL in the crude membrane fraction it was clear that while it  
3 did not completely denude MLKL of ubiquitin, the WT USP21-CaaX fusion did substantially  
4 reduce the amount of ubiquitylated MLKL, as well as generally affecting the levels of  
5 ubiquitylated proteins (**Fig. 3B**). Taken together these data suggest that ubiquitylated MLKL  
6 is localised to the plasma membrane.

7

### 8 **Necroptosis induced MLKL ubiquitylation is driven by its oligomerization**

9 In order to kill, MLKL oligomerizes, translocates to, and permeabilises membranes. To  
10 dissect further the drivers of MLKL ubiquitylation, we generated a series of MLKL mutants  
11 that were defective in one or more of these essential steps. Previously, we found that alanine  
12 replacement of the surface exposed residues R105 and D106 in the four-helix bundle (4HB)  
13 domain of mouse MLKL prevents it from oligomerising, translocating and inducing cell  
14 death (Hildebrand *et al.*, 2014; Tanzer *et al.*, 2016). In the context of full length MLKL, we  
15 found that these mutations prevent formation of a high molecular weight complex (complex  
16 II) in the ‘crude membrane’ fraction following necroptotic stimulation by TSQ (**Fig. 4A**).  
17 Although R105A/D106A MLKL was phosphorylated following this necroptotic stimulus, it  
18 did not exhibit the distinct TSI-induced ubiquitylation observed for WT MLKL (**Fig. 4B**).  
19 This supports the idea that MLKL only undergoes ubiquitylation post activation by RIPK3  
20 and suggests that MLKL does not undergo ubiquitylation without oligomerization.

21

22 The MLKL mutants, Q343A (which perturbs a hydrogen bond with K219 in the ATP binding  
23 motif VTIK) and S345D (phospho-mimetic), are auto-activated forms of murine MLKL  
24 (Murphy *et al.*, 2013). We induced expression of Q343A or S345D mutant MLKL in *Mlkl*<sup>-/-</sup>  
25 and *Ripk3*<sup>-/-</sup>*Mlkl*<sup>-/-</sup> MDFs for 16 hrs where, as predicted, they killed cells independently of an  
26 extrinsic necroptotic stimulus (**Supp. Fig. 4B**). As expected, induction of necroptosis in  
27 *Mlkl*<sup>-/-</sup> cells reconstituted with wild type MLKL resulted in MLKL ubiquitylation (**Fig. 4C**).  
28 However, activated MLKL mutants expressed in the same *Mlkl*<sup>-/-</sup> MDFs were ubiquitylated  
29 independently of a necroptotic stimulus and to an extent comparable to wildtype MLKL  
30 induced to undergo necroptosis (**Fig. 4C**). Furthermore, Q343A MLKL became ubiquitylated  
31 in *Ripk3*<sup>-/-</sup>*Mlkl*<sup>-/-</sup> MDFs and therefore independently of any upstream activation (**Fig. 4D**). We  
32 conclude that while MLKL ubiquitylation correlates with its oligomerization and  
33 phosphorylation, direct RIPK3 association is not required for MLKL ubiquitylation in murine  
34 cells.



1

2 Necrosulfonamide (NSA) is an inhibitor of human MLKL by forming a covalent bound with  
3 Cys86 that only exists in human MLKL but not mouse MLKL (Liu *et al.*, 2017). Consistent  
4 with a recent report (Murai *et al.*, 2018; Samson *et al.*, 2020), we found that while it did not  
5 inhibit the phosphorylation of MLKL or the formation of high molecular weight MLKL-  
6 containing complex, large proportions of this MLKL species remained in the cytosolic (0.025%  
7 digitonin soluble) fraction (C) of cells (**Fig. 4E**). Consistent with the reduction in MLKL  
8 oligomer in the crude membrane (0.025% digitonin insoluble) fraction (M), NSA also  
9 reduced MLKL ubiquitylation (**Fig. 4F**).

10

### 11 **Ubiquitylated MLKL undergoes proteasome and lysosome dependent turnover**

12 Unlike the R105A/D106A MLKL mutant, E109A/E110A MLKL mutant and N-terminal  
13 FLAG-tagged MLKL (N-FLAG MLKL) are able to form higher order oligomers in crude  
14 membrane fractions following necroptotic stimulation, yet are nevertheless unable to induce  
15 necroptosis (Hildebrand *et al.*, 2014; Tanzer *et al.*, 2016) (**Fig. 5, B, Supp. Fig. 5A, B**).  
16 These mutants therefore allowed us to examine whether ubiquitylation was a consequence of  
17 necroptosis. Upon induction of necroptosis, E109A/E110A MLKL was more heavily  
18 phosphorylated and ubiquitylated than wildtype MLKL (**Fig. 5C**). Similarly, N-FLAG  
19 MLKL was also phosphorylated and ubiquitylated within 2 hrs of TSI treatment, although  
20 these modified MLKL species diminished over time (**Fig. 5D**).

21

22 The cellular turnover of active forms of MLKL has been observed previously by our group  
23 and by others (Gong *et al.*, 2017; Hildebrand *et al.*, 2020; Yoon *et al.*, 2017; Zargarian *et al.*,  
24 2017). Therefore, we examined ubiquitylation of N-FLAG MLKL in MDFs over a time  
25 course following a TSI pulse. N-FLAG MLKL is phosphorylated, oligomerizes and  
26 accumulates in the 0.025% insoluble cell fraction without killing *Mkl1*<sup>-/-</sup> MDFs following  
27 necroptotic stimulation. This later feature facilitates the study of these ubiquitylated MLKL  
28 species and their cellular turnover *in situ* using proteasome and lysosome inhibitors as  
29 previously described for unmodified MLKL (Hildebrand *et al.*, 2020). We found that after 4  
30 hrs TSI stimulation, levels of ubiquitylated and phosphorylated N-FLAG MLKL dramatically  
31 decreased. This decrease can be delayed by either the lysosome inhibitor bafilomycin or the  
32 proteasome inhibitor PS341 (**Fig. 5E**). This suggests that MLKL ubiquitylation correlates  
33 with its proteasome and lysosome dependent turnover.

34

## 1 **MLKL ubiquitylation antagonises necroptosis**

2 We sought to identify the precise amino acids on MLKL that were modified by ubiquitin. We  
3 enriched for activated and ubiquitylated N-FLAG MLKL from the ‘crude membrane’ fraction  
4 of MDFs by performing a FLAG tag affinity purification. Eluted fractions from FLAG  
5 affinity beads were analysed by mass spectrometry, which identified Gly-Gly conjugates on  
6 lysine residues K9, K51, K69 and K77 (**Supp. Fig. 6A**). All four are located in the 4HB  
7 domain of MLKL (**Supp. Fig. 6B**) which suggests a role for ubiquitylation in regulating  
8 MLKL-mediated cell death. We did not identify any additional signs of ubiquitin  
9 modification on the brace or pseudokinase region of MLKL using this experimental system.

10

11 We mutated the four lysines to arginine and inducibly expressed the “4KR” mutant in *Mkl<sup>-/-</sup>*  
12 MDFs to explore their role. Surprisingly, the 4KR MLKL was phosphorylated and  
13 ubiquitylated in a similar manner to wild type MLKL following TSI treatment (**Fig. 6B**).  
14 There was a reduction in the ability of this mutant to kill cells in response to TSI treatment  
15 (**Supp. Fig. 6C**), but this is seemingly unrelated to its ubiquitylation and more likely due to  
16 modification of conserved residues in the cytotoxic domain of MLKL. These results highlight  
17 the difficulties in mutational analyses when studying ubiquitylation and rather than mutate  
18 any of the other 38 lysines in MLKL we tried a different approach.

19

20 We had observed that the deubiquitylating enzyme USP21 removed all ubiquitin from MLKL  
21 *in vitro* (**Fig. 2B**). We therefore hypothesised that fusing the catalytic domain of USP21 to  
22 MLKL would remove TSI induced ubiquitylation from MLKL. We fused it to the C-terminal  
23 end of MLKL, because, as with the FLAG tag, N-terminal fusions affect the ability of MLKL  
24 to kill (**Supp. Fig. 5A**). We fused the catalytic domain of USP21 to the C-terminus of both  
25 human and mouse MLKL (**Fig. 7A**) and expressed the fusion proteins in *MLKL<sup>-/-</sup>* HT29 and  
26 *Mkl<sup>-/-</sup>* MDF cells respectively, to determine, firstly, whether it still retained cytotoxic activity  
27 and, secondly, whether it would be resistant to necroptosis induced ubiquitylation. To  
28 specifically control for the loss of ubiquitylation, we also generated MLKL fused to a  
29 catalytically-dead USP21 mutant (USP21<sup>C221R</sup>; **Fig. 7A**), as mentioned in **Fig. 3B**. Both the  
30 MLKL-USP21 and MLKL-USP21<sup>C221R</sup> fusion proteins were exogenously expressed and the  
31 cells were stimulated with TSI for varying amounts of time. Ubiquitylated proteins were  
32 enriched *via* UBA-pulldown. Like murine MLKL<sup>WT</sup>, the catalytically inactive control,  
33 MLKL-USP21<sup>C221R</sup>, when expressed in *Mkl<sup>-/-</sup>* MDFs, showed high MW laddering indicative  
34 of ubiquitylation and the ubiquitylation was enhanced following TSI stimulation (**Fig. 7B**).

1 These high MW MLKL-USP21<sup>C221R</sup> species were reduced and collapsed into non-  
2 ubiquitylated form by digestion of recombinant USP21 (**Supp. Fig 7C**). In contrast, the  
3 ubiquitin laddering was not evident for the MLKL-USP21<sup>WT</sup> fusion (**Fig. 7B**). MLKL-USP21  
4 and MLKL-USP21<sup>C221R</sup> re-constituted sensitivity to TSI stimulation in *Mkl1*<sup>-/-</sup> MDFs with  
5 only modestly delayed kinetics when compared to wildtype MLKL (**Fig. 7C**). However,  
6 unlike wildtype MLKL or MLKL-USP21<sup>C221R</sup>, MLKL-USP21 could induce cell death  
7 independent of TSI stimulation (**Fig. 7C**), even when expressed in *Ripk3*<sup>-/-</sup>*Mkl1*<sup>-/-</sup> MDFs (**Fig.**  
8 **7C**), without being phosphorylated (see Input fractions in **Supp. Fig. 7C**).

9  
10 We made similar observations for human MLKL-USP21 fusions expressed in *MLKL*<sup>-/-</sup> HT29  
11 cells. Human MLKL-USP21<sup>C221R</sup>, but not MLKL-USP21 fusions, became ubiquitylated  
12 following TSI stimulation (**Fig. 7E**). Furthermore, like human MLKL, human MLKL-USP21  
13 and MLKL-USP21<sup>C221R</sup> fusions were able to reconstitute the capacity of *MLKL*<sup>-/-</sup> HT29 cells  
14 to undergo TSI induced necroptosis when their expression was induced by doxycycline (**Fig.**  
15 **7D**), while USP21 controls did not (**Supp. Fig. 7B**). For the first 10 hrs of expression and  
16 activation, NSA blocked TSI-induced cell death for all MLKL species, which was then  
17 overcome by overexpression. MLKL-USP21 also exhibited TSI-independent cell death,  
18 occurring from 16 hrs, which can also be delayed by NSA. (**Fig. 7D**). While  
19 phosphorylated MLKL was not detected by that time (**Fig. 7E**). These data indicate that  
20 ubiquitylation of MLKL is not required for necroptotic cell death, but rather acts as an  
21 important kinetic regulator of the necroptosis pathway following oligomerization and  
22 membrane association.

## 24 **Discussion**

25 MLKL undergoes ubiquitylation during necroptosis. In this study, we identified distinctive  
26 ubiquitylation of both mouse and human MLKL that could be induced by a range of  
27 necroptotic stimuli. This signature ubiquitin ladder was essentially resistant to cleavage by a  
28 host of DUBs. Only USP21, the DUB that can remove all ubiquitin modifications, including  
29 mono-ubiquitylation, was able to deubiquitylate MLKL. Therefore, we propose that MLKL is  
30 mono-ubiquitylated at multiple sites. Mono-ubiquitylation is typically associated with  
31 endosome-lysosome trafficking (Haglund *et al*, 2003; Mosesson & Yarden, 2006) and is less  
32 likely to play a scaffolding role or result in proteasomal degradation (Oh *et al*, 2018;  
33 Wilkinson *et al*, 1995).

1  
2 Full activation of MLKL's killing activity is a multi-step and protracted process, the  
3 choreography of which has not yet been fully deduced. Nevertheless there is a broad  
4 consensus, based on analysis of MLKL mutants and a range of different techniques, that  
5 phosphorylation by RIPK3 leads to MLKL oligomerization, translocation to biological  
6 membranes and subsequent membrane permeabilization (Petrie *et al.*, 2020; Petrie *et al.*, 2018;  
7 Samson *et al.*, 2020; Tanzer *et al.*, 2016). Recent single-cell imaging approaches examining  
8 human MLKL show that phosphorylated MLKL clusters in cytoplasmic vesicles together  
9 with RIPK1. These vesicles are actively transported to the plasma membrane, where they  
10 begin to coalesce in hotspots, some hours prior to membrane lysis (Samson *et al.*, 2020).  
11 Consistent with data showing that NSA does not prevent MLKL phosphorylation or initial  
12 oligomerization, but does block higher order oligomerization (Liu *et al.*, 2017)), NSA  
13 appears to prevent MLKL clustering (Samson *et al.*, 2020). To define where and when  
14 ubiquitylation of MLKL occurred we fractionated cells into cytosolic and crude membrane  
15 fractions, and only detected ubiquitylated MLKL in the 0.025% digitonin insoluble (crude  
16 membrane) fraction. We also examined a number of different MLKL mutants that we had  
17 previously characterised for their ability to form oligomers, translocate to the crude  
18 membrane fraction and promote necroptosis. The MLKL mutants, Q343A and S345D, which  
19 are able to form 0.025% digitonin insoluble high molecular weight oligomers and induce cell  
20 death without necroptotic stimulation (Murphy *et al.*, 2013; Tanzer *et al.*, 2015), were  
21 ubiquitylated independently of RIPK3 or a necroptotic TSQ stimulus. On the other hand, the  
22 R105A/D106A mutant that is unable to form high molecular weight oligomers on BN-PAGE  
23 did not become ubiquitylated following a necroptotic stimulus. This implies that MLKL  
24 ubiquitylation occurs after MLKL oligomerization and does not specifically require RIPK3 or  
25 upstream signalling.

26  
27 MLKL has been variously reported to traffic to the nucleus (Weber *et al.*, 2018; Yoon *et al.*,  
28 2016), lysosomes (Fan *et al.*, 2019; Wang *et al.*, 2014; Yoon *et al.*, 2017), mitochondria  
29 (Wang *et al.*, 2012) and the plasma membrane (the most likely location) (Cai *et al.*, 2014;  
30 Chen *et al.*, 2014; Hildebrand *et al.*, 2014; Samson *et al.*, 2020) following necroptotic  
31 activation. Crude membrane fractionation enriches membrane and insoluble protein  
32 aggregates, therefore in an attempt to determine more precisely where MLKL ubiquitylation  
33 occurred, we generated a plasma membrane-targeted, CaaX-fused USP21 (Wright & Philips,  
34 2006). Because ubiquitin modification plays a role in the initial, plasma membrane located,

1 TNF/TNFR1 induced necroptotic signalling, we anticipated that expressing USP21-CaaX  
2 might affect induction of necroptosis. However necroptosis was induced in cells expressing a  
3 non-targeted USP21 or a catalytically inactive USP21<sup>C221R</sup>-CaaX to equal levels as in  
4 USP21-CaaX cells, despite the fact that USP21-CaaX was clearly active and reduced total  
5 ubiquitin levels. Consistent with MLKL being targeted to the plasma membrane, MLKL was  
6 less ubiquitylated in USP21-CaaX cells than in cells expressing USP21<sup>C221R</sup>-CaaX following  
7 a necroptotic stimulus. MLKL ubiquitylation was, however, not completely prevented by  
8 USP21-CaaX expression leaving open several interpretations of this data viz: not all MLKL  
9 is ubiquitylated at the plasma membrane; or USP21-CaaX was unable to access all MLKL in  
10 the membrane; or MLKL is ubiquitylated prior to reaching the plasma membrane and can  
11 only be deubiquitylated once it arrives there. Therefore while we cannot exclude that  
12 ubiquitylated MLKL sediments as part of large amyloid-like polymers or large cytoskeletal  
13 structures in the crude membrane fraction without being directly associated with a biological  
14 membrane (Liu *et al.*, 2017), our data suggest that at least some ubiquitylated MLKL is  
15 accessible to a plasma membrane localised DUB.

16

17 As previously observed (Murai *et al.*, 2018), we found that in the presence of NSA, the high  
18 molecular weight human MLKL complex that is normally found exclusively in the crude  
19 membrane fraction was now also observed in the cytosolic fraction. Combined with other  
20 observations (Samson *et al.*, 2020), this indicates that NSA interferes with MLKL membrane  
21 association. Since NSA treatment also inhibited MLKL-ubiquitylation, this suggests that  
22 membrane association is required for MLKL ubiquitylation, and that the relevant E3 ligase is  
23 also membrane associated.

24

25 Neither N-terminally FLAG tagged MLKL nor the E109A/E110A mutant MLKL are capable  
26 of killing cells, although both are phosphorylated and form 0.025% digitonin-insoluble high  
27 molecular weight oligomers in a similar manner to wild type MLKL following induction of  
28 necroptosis. Since both are also ubiquitylated we can conclude that ubiquitylation is not  
29 sufficient to cause necroptosis. To more precisely define the role of MLKL ubiquitylation  
30 during necroptosis we used mass spectrometry to identify ubiquitylated lysines in mouse  
31 MLKL. We found four such lysines in the 4HB domain, but none in the pseudokinase domain.  
32 Only one of these four, K77, is conserved in human MLKL, however this is not particularly  
33 surprising because homology of charged residues in MLKL is not well conserved between  
34 mouse and human (**Supp. Fig. 6B**).

1  
2 Mutation of these lysines did not prevent either MLKL induced killing or MLKL  
3 ubiquitylation. The persistence of ubiquitin modification is a relatively common scenario  
4 when trying to define the role of ubiquitylation by mutating lysine. This is because E3 ligase  
5 mediated ubiquitylation is rarely tightly restricted to a motif and can therefore be  
6 promiscuous in target modification (Petroski & Deshaies, 2003; Wu *et al*, 2003). This means  
7 that if a favoured lysine in the target is mutated, the E3 ligase may nevertheless ubiquitylate  
8 another lysine. We therefore tried a more innovative approach. Since we had shown that the  
9 DUB USP21 was able to remove necroptosis induced ubiquitylation of MLKL *in vitro*, we  
10 generated an MLKL C-terminal USP21 fusion that we predicted would be constitutively  
11 deubiquitylated. A similar approach fusing the K63 specific DUB AMSH to EGFR has been  
12 used to investigate EGFR degradation (Huang *et al*, 2013), however it was not clear whether  
13 a DUB that removes all ubiquitin would be as well tolerated by cells. Stable inducible  
14 expression of USP21 alone was not toxic to cells over 24 hours and fusion of the wildtype or  
15 catalytically-dead USP21 did not markedly affect MLKL's cytotoxic activity following a TSI  
16 death stimulus. Furthermore, catalytically-active USP21 fused to MLKL prevented TSI  
17 induced ubiquitylation of MLKL. Interestingly, in both human and mouse cells, loss of  
18 MLKL ubiquitylation also allowed MLKL to kill cells without a necroptotic stimulus, albeit  
19 less potently when compared with such a stimulus. This further supports the idea that  
20 ubiquitylation of MLKL is an important 'insurance policy' against low level activation of  
21 MLKL by other cellular kinases or low level spontaneous transition to the active  
22 conformation. Furthermore our results indicate that the approach of directly fusing a DUB,  
23 even a pan DUB like USP21, to a protein of interest may be a widely applicable technique to  
24 evaluate the role of ubiquitin modification in other systems.

25  
26 Other mechanisms have been proposed for MLKL turnover post-activation. The ESCRT-III  
27 machinery was proposed to mediate plasma membrane shedding alongside active MLKL  
28 during necroptosis (Gong *et al.*, 2017), and cells were reported to release active MLKL  
29 containing vesicles via endosomal trafficking (Fan *et al.*, 2019; Yoon *et al.*, 2017; Zargarian  
30 *et al.*, 2017). It has been proposed that this turnover helps set a threshold of activated MLKL  
31 required for necroptosis and that it delays the onset of cell death to allow production of  
32 essential cytokines and Damage-associated molecular patterns (DAMPs) and an  
33 inflammatory response (Vandenabeele *et al*, 2017). Another possibility is that the prolonged  
34 multi-step path from MLKL phosphorylation to membrane permeabilization and cell death



1 allows multiple points of regulation that ensure that a cell only commits to necroptosis under  
2 precisely defined conditions (Dovey *et al.*, 2018; Hildebrand *et al.*, 2020; Jacobsen *et al.*, 2016;  
3 Samson *et al.*, 2020). For this to work, the cell must have mechanisms to deactivate already  
4 activated MLKL, and the ubiquitylation of MLKL may serve as one such mechanism. Our  
5 results, showing that MLKL-USP21, but not a wild type MLKL expressed to similar levels,  
6 kills cells in the absence of a necroptotic stimulus suggest that MLKL may be continually  
7 translocating to membranes and turned over by MLKL-ubiquitylation. Like the rapid  
8 degradation of inflammatory cytokine mRNAs (Lacey *et al.*, 2015; Menon & Gaestel, 2018)  
9 although energetically costly, this might allow a more rapid response to a pathogen than an  
10 on/off mechanism focused solely on initiation and may also provide another mechanism to  
11 detect and act on attempts by pathogens to interfere with this anti-pathogen response.

12

## 13 **Materials and Methods**

14

### 15 **Compounds and cytokines**

16 Human TNF-Fc made in-house, Smac-mimetics Compound A (Tetralogic), IDN-6556  
17 (Tetralogic), Q-VD-OPh (R & D Systems), Lipopolysaccharide (LPS, Sigma), Poly I:C  
18 (Sigma), Fas Ligand (a gift from Lorraine O'Reilly, WEHI), doxycycline (Sigma),  
19 Necrostatin-1 (Nec-1, Sigma), GSK872 (a gift from Anaxis Pty, Ltd.), coumermycin (Sigma),  
20 Necrosulfonamide (NSA, Merck Millipore), Propidium iodide (Sigma), Sytox Green  
21 (Thermo Fisher), puromycin (Thermo Fisher), N-ethylmaleimide (NEM, Sigma),  
22 deubiquitylase (DUBs) made in house (Hospenthal *et al.*, 2015), complete protease inhibitor  
23 cocktail (Roche), Bafilomycin A1 (BAF, Enzo), PS341 (Sigma).

24

### 25 **Antibodies:**

26 Mouse phospho-MLKL (Ser345) rabbit monoclonal ERP9515(2) (Abcam)  
27 Mouse phospho-MLKL (Ser345) rabbit monoclonal (D6E3G) (Cell Signalling Technology)  
28 MLKL rat monoclonal 3H1 (available from Millipore MABC604; generated in-house)  
29  $\beta$ -actin mouse monoclonal AC-15 (Sigma A-1978)  
30 BAK NT rabbit polyclonal #06-536 (EMD Millipore)  
31 GAPDH rabbit monoclonal 14C10 (Cell Signalling Technology)  
32 Pan-ubiquitin mouse monoclonal #3939 (Cell Signalling Technology)  
33 Mouse/human RIPK1 mouse monoclonal #610458 (BD transduction Laboratories)

- 1 Mouse RIPK3 rabbit polyclonal PSC-2283-c100 (Axxora (Pro Sci))
- 2 Human RIPK3 rat monoclonal 1H2 (generated in-house)(Petrie *et al.*, 2019b)
- 3 Human phospho-MLKL (Ser358) rabbit monoclonal ab 187091 (Abcam)
- 4 VDAC1 rabbit polyclonal AB10527 (Millipore)
- 5 Human Usp21 rabbit polyclonal 17856-I-AP (Proteintech)
- 6 HRP-conjugated secondary antibodies

7

## 8 **Cell lines immortalization and transfection**

9 Cells were cultured in DMEM+8% FCS at 37°C. HT29 cells were a kind gift from Mark  
10 Hampton. MDFs were isolated from tails of mice bearing different genotype, and  
11 immortalized by SV40 large T antigen via lentivirus transduction. MLKL mutant constructs  
12 were generated as described previously ((Hildebrand *et al.*, 2014; Moujalled *et al.*, 2014;  
13 Murphy *et al.*, 2013)). All oligonucleotides for PCR and mutagenesis were synthesized by  
14 IDT. Constructs encoding USP21 catalytic domain with GS linker were made by GenScript  
15 (Nanjing, CN). Genes encoding WT mouse MLKL and PCR-derived mutants were cloned  
16 into pF TRE3G PGK puro, a puromycin-selectable, doxycycline-inducible vector as  
17 previously described (and kindly supplied by Toru Okamoto) (Hildebrand *et al.*, 2014;  
18 Moujalled *et al.*, 2014; Murphy *et al.*, 2013; Tanzer *et al.*, 2016). Lentiviruses were generated  
19 in HEK293T cells before infection of target cells. Puromycin (5 µg/mL) was added for  
20 selection and maintenance of lines stably transduced with lentivirus.

21

22 For BMDMs, femora and tibiae were collected from WT and *Tnf*<sup>-/-</sup> mice at 6 weeks old, cut  
23 and flushed by PBS. Bone marrow were incubated in Petri dishes with DMEM supplemented  
24 with 10% FCS and 20% conditioned L929 medium for 7 days. Cells were fed with fresh  
25 medium after 3 days of plating.

26

## 27 **Concentrations of stimuli and inhibitors**

28 TNF (100 ng/mL), Smac-mimetic Compound A (500 nM), IDN-6556 (5 µM), Q-VD-OPh (5  
29 µM), doxycycline (20 ng/mL), Necrostatin-1 (50 µM), GSK872 (5 mM), LPS (50 ng/mL),  
30 Fas ligand (6.4 ng/mL), Poly I:C (1 mg/mL), coumermycin (700 nM), Bafilomycin (5 µM),  
31 PS341 (50 nM), MG132 (200nM), Chloroquine (50 µM), NH<sub>4</sub>Cl (2 mM), Ca-074 Me (20  
32 µM), TLCK (100 µM), AEBSF (100 µM) and concentrations otherwise indicated.

33



1 **Cell death measured by flow cytometry**

2 Cells were plated at 50,000/well in 24-well plates before treatment, collected by trypsin and  
3 spun down, resuspended and stained with PI (Propidium Iodide, 1 µg/mL) in PBS buffer, and  
4 quantified by Flow cytometry.

5

6 **Cell death measured by live cell imaging**

7 MDFs were plates at 10,000/well or 15,000/well (96-well plates) and HT29s were plated at  
8 40,000/well (48-well plates) or 15,000/well (96-well plates) and allowed to settle for 4 hrs  
9 (MDFs) and 24 hrs (HT29s) respectively. Cells were stimulated as indicated in media  
10 containing Propidium Iodide (PI, 200 ng/mL) or Sytox Green (500nM, ThermoFisher  
11 Scientific) and imaged at 45 min or 1 hr intervals using an IncuCyte S3 Live cell imager.  
12 Numbers of PI or Sytox positive cells were quantified and plotted using IncuCyte software.

13

14 **Cellular fractionation and Blue Native-PAGE**

15 Cells were collected by scraping, spun down and washed in pre-chilled PBS. MELB buffer  
16 (20 mM 4-(2-Hydroxyethyl) piperazine-1-ethanesulfonic acid, (HEPES) pH=7.5, 100 mM  
17 sucrose, 2.5 mM MgCl<sub>2</sub>, 100 mM KCl) containing 0.025% digitonin was used to  
18 permeabilise cells to extract the cytosol fraction. Non-soluble part was further solubilized by  
19 1% digitonin buffer. (Liu *et al.*, 2018; Schagger & von Jagow, 1991) Both fractions were  
20 separated by Bis-Tris Native PAGE, and transferred to PVDF membrane. After transfer the  
21 membrane was then destained (50% methanol and 25% acetic acid) and denatured (in 6M  
22 guanidine HCl, 5 mM β-ME) to maximise epitope exposure.

23

24 **UBA-pull down assay and UbiCRest**

25 Recombinant GST-UBA fusion protein (Hjerpe *et al.*, 2009) purified from *E. coli* in house  
26 was prebound to glutathione sepharose beads (10 µL/condition). Cells were lysed in DISC  
27 buffer (30 mM Tris-HCl, pH 7.5, 150 mM NaCl, 10% glycerol) containing 1% Triton X-100  
28 with 10 mM NEM and protease inhibitor. Cleared lysate was then coupled with beads  
29 overnight. SDS-PAGE sample loading buffer was used to elute the UBA-pull down fraction.  
30 For UbiCrest, washed beads were then incubated with DUBs at previously established  
31 concentrations (Hospenthal *et al.*, 2015) and incubated at 37°C for the indicated times.  
32 Digestion product was eluted in SDS sample buffer for Western blot analysis. Beads elution

1 fractions were generated by removing the digestion product from the beads and following  
2 washing.

3

#### 4 **FLAG-tagged protein immunoaffinity precipitation and Mass Spectrometry sample** 5 **preparation**

6 N-FLAG WT mouse MLKL was inducibly expressed in *Mlkl*<sup>-/-</sup> MDFs by doxycycline  
7 overnight and stimulated with TSI for 3 hrs. Cells were collected by scraping and  
8 permeabilised by 0.025% digitonin in MELB buffer together with NEM (10 mM) and  
9 protease inhibitors. The crude membrane fraction was pelleted by centrifugation and  
10 dissolved in 1% SDS in DISC buffer. Cleared lysate of crude membrane was then applied to  
11 M2-FLAG beads for affinity precipitation. FLAG tagged protein on beads was eluted by  
12 heating at 56°C in 0.5% SDS solution. Eluted material was subjected to tryptic digestion  
13 using the FASP method (Wisniewski *et al*, 2009). Peptides were lyophilised using CentriVap  
14 (Labconco) prior to reconstituting in 80 µl 0.1% FA/2% acetonitrile (ACN). Peptide mixtures  
15 (1 µl) were analysed by nanoflow reversed-phase liquid chromatography tandem mass  
16 spectrometry (LC-MS/MS) on an M-Class HPLC (Waters) coupled to a Q-Exactive Orbitrap  
17 mass spectrometer (Thermo Fisher). Peptide mixtures were loaded in buffer A (0.1% formic  
18 acid, 2% acetonitrile, Milli-Q water), and separated by reverse-phase chromatography using  
19 C<sub>18</sub> fused silica column (packed emitter, I.D. 75 µm, O.D. 360 µm x 25 cm length,  
20 IonOpticks, Australia) using flow rates and data-dependent methods as previously described  
21 (Delconte *et al*, 2016; Kedzierski *et al*, 2017). Raw files consisting of high-resolution  
22 MS/MS spectra were processed with MaxQuant (version 1.5.8.3) for feature detection and  
23 protein identification using the Andromeda search engine (Cox *et al*, 2011). Extracted peak  
24 lists were searched against the UniProtKB/Swiss-Prot *Mus musculus* database (October 2016)  
25 and a separate reverse decoy database to empirically assess the false discovery rate (FDR)  
26 using strict trypsin specificity allowing up to 2 missed cleavages. The minimum required  
27 peptide length was set to 7 amino acids. The mass tolerance for precursor ions and fragment  
28 ions were 20 ppm and 0.5 Da, respectively. The search included variable modifications of  
29 oxidation (methionine), amino-terminal acetylation, carbamidomethyl (cysteine), GlyGly or  
30 ubiquitylation (lysine), phosphorylation (serine, threonine or tyrosine) and N-ethylmaleimide  
31 (cysteine).

32

#### 33 **Data availability**

1 The raw mass spectrometric data and the MaxQuant result files have been deposited to the  
2 ProteomeXchange Consortium via the PRIDE (Perez-Riverol *et al*, 2019) partner repository  
3 with the dataset identifier: PXD015537.

4 Username: [reviewer27536@ebi.ac.uk](mailto:reviewer27536@ebi.ac.uk) Password: f2WTYnC4

5

#### 6 **Acknowledgements:**

7 We would like to thank Jiami Han, Yueyuan Li and the WEHI mouse facility for technical  
8 assistance. This work was funded by NHMRC grants 1025594 (JS), 1046984 (JS) and  
9 1105023 (JS and JMH) and fellowships 1172929 (JMM), 1058190 (JS), 1107149 (JS) and  
10 110574 (JS) and was made possible through Victorian State Government Operational  
11 Infrastructure Support and Australian Government NHMRC IRIISS (9000587).

12

#### 13 **Author Contribution**

14 ZL, LD and KSA designed and performed experiments, and analysed data. ZL, JMH and JS  
15 analysed the data and wrote the manuscript. DK conceived the DUB fusion experiment and  
16 provided reagents. All authors read and commented on the manuscript.

17

#### 18 **Conflict of interest statement**

19 SNY, AB, UN, CF, SEG, JMM, JMH and JS contribute to, or have contributed to, a project  
20 with Anaxis Pty Ltd to develop necroptosis inhibitors.

21

1 **Figure legends**

2

3 Abbreviations: TNF (T), Smac-mimetics Compound A (S), IDN-6556 (I), Q-VD-OPh (Q),  
4 whole cell lysate (WCL), GST-UBA pull down fractions (UBA-PD), cytosolic fraction (C),  
5 crude membrane fraction (M), wildtype (WT), C221R (CR), Propidium Iodide (PI),  
6 Necrostatin-1 (Nec-1), ubiquitin (Ub) and others as indicated elsewhere. TS, SI, TSI and TSQ  
7 are used in combination, as apoptotic or necroptotic stimuli.

8

9 **Figure 1. MLKL undergoes ubiquitylation during necroptosis**

10

11 A WT MDFs were treated  $\pm$  TSI individually or in combination for 3 hrs. Whole cell lysates  
12 (WCL) and UBA-pull down (UBA-PD) fractions were analysed by Western blot and  
13 probed with antibodies as indicated. Representative of three independent experiments.  
14 Samples of UBA-pull down in following figures were analysed in the same way unless  
15 otherwise indicated.

16 B WT, *Ripk3*<sup>-/-</sup>, *Mkl1*<sup>-/-</sup>, *Tnfr1*<sup>-/-</sup> and *Traf2*<sup>-/-</sup> MDFs were untreated (UT) or treated with TSI  
17 for 3 hrs. Nec-1 and GSK872 were added to inhibit RIPK1 and RIPK3 kinase activities  
18 respectively.

19 C WT and *Tnf*<sup>-/-</sup> BMDMs were treated  $\pm$  death ligands including TNF (T), LPS (L), Fas  
20 ligand (F) and Poly I:C (P) in addition to S and I for 3 hrs.

21 D WT HT29 cells were untreated (UT) or treated with TSI for 16 hrs.

22 E RIPK3-gyrase were inducibly expressed in *Ripk3*<sup>-/-</sup> MDFs by doxycycline (dox) for 5 hrs,  
23 and cells were then treated  $\pm$  combination of TSI, or coumermycin (coum) for 3 hrs.

24

25 **Supplementary Figure 1. Cell death time course of MDFs and HT29 cells following**  
26 **necroptotic stimulation**

27

28 MDFs (A) and HT29 (B) cells were treated with TSI. Cell death was measured by PI staining  
29 and flow cytometry. Data are plotted as mean  $\pm$  SEM of three independent experiments.

30

31

1 **Figure 2. MLKL is mono-ubiquitylated at multiple sites**

2

3 A Deubiquitylating enzymes (DUBs) and their ubiquitin substrates. Less efficiently cleaved  
4 substrates are indicated in brackets.

5 B UBA-pull down from WT MDFs treated with TSI for 3 hrs were subjected to the DUBs  
6 shown in (A). Beads eluates were analysed by Western blot and probed with antibodies as  
7 indicated. Representative of three independent experiments.

8 C 1.4 mL cleared cell lysate from  $4 \times 10^6$  TSI-treated WT MDFs was split into three parts of  
9 the indicated volume, followed by UBA-pull down and DUB incubation. Bead eluates  
10 were analysed by Western blot and probed with the indicated antibodies. Representative of  
11 three independent experiments.

12

13

14 **Figure 3. MLKL ubiquitylation accumulates in the crude membrane fraction and can**  
15 **be digested by USP21 located on biological membranes.**

16

17 A WT MDFs were treated with TSI for indicated time. Cells were fractionated into cytosol  
18 and crude membrane parts, followed by UBA-pull down. All fractions were analysed by  
19 Western blot and probed with antibodies as indicated. Representative of three independent  
20 experiments.

21 B WT USP21-CaaX and USP21<sup>C221R</sup>-CaaX (CR) were inducibly expressed in WT MDFs by  
22 doxycycline for 5 hrs. Ubiquitylated proteins were enriched followed by TSI stimulation  
23 and cellular fractionation. All fractions were analysed by Western blot and probed with  
24 antibodies as indicated. Representative of three independent experiments.

25

26 **Supplementary Figure 3. USP21-CaaX expression does not alter the kinetics of TNF**  
27 **induced apoptosis or necroptosis in MDFs.**

28

29 A WT USP21, USP21-CaaX and USP21<sup>C221R</sup>-CaaX were inducibly expressed in WT MDFs  
30 by doxycycline. TS and Nec-1 were used to control for apoptotic signalling. Sytox Green  
31 positive cells were quantified in real time by live cell imaging. Representative of 2  
32 independent experiments.

33

1 **Figure 4. MLKL oligomerization drives its necroptosis specific ubiquitylation**

2

3 A WT and R105AD106A mutant MLKL were inducibly expressed in *Mlkl*<sup>-/-</sup> MDFs by  
4 doxycycline, at the same time cells were untreated (UT) or treated with for 6 hrs. Cells  
5 were fractionated into cytosol (C) and crude membrane (M). Fractions were analysed by  
6 BN- or SDS-PAGE, Western blot and probed with the indicated antibodies.  
7 Representative of three independent experiments.

8 B Cell lysates from (A) were subjected to UBA-pull down and analysed as described above.

9 C WT, Q343A and S345D mutant MLKL were inducibly expressed in *Mlkl*<sup>-/-</sup> MDFs by  
10 doxycycline, at the same time cells were treated ± TSQ for 16 hrs, followed by UBA-  
11 pulldown. Representative of three independent experiments.

12 D WT and Q343A mutant MLKL were inducibly expressed in *Ripk3*<sup>-/-</sup>*Mlkl*<sup>-/-</sup> MDFs by  
13 doxycycline, at the same time cells were treated ± TSQ for 16 hrs, followed by UBA-  
14 pulldown. Representative of three independent experiments.

15 E HT29 cells were stimulated with TSI, ± NSA (500 nM), or left untreated (UT) for 16 hrs,  
16 followed by cellular fractionation. Fractions were analysed by BN- or SDS-PAGE,  
17 Western blot and probed with the indicated antibodies. Representative of three  
18 independent experiments.

19 F Cell lysates from (E) were subjected to UBA-pulldown and analysed as described above.

20

21 **Supplementary Figure 4. MLKL oligomerization drives its necroptosis specific**  
22 **ubiquitylation**

23

24 A Cell death of samples from **Fig. 4A** was measured by PI staining based on flow cytometry.

25 Data are plotted as mean ± SEM of three independent experiments.

26 B Cell death of samples from **Fig. 4C, D** were analysed as in (A).

1 **Figure 5. MLKL-ubiquitylation does not lead to cell death, but correlates with the**  
2 **turnover of activated MLKL**

3

4 A WT and E109AE110A mutant MLKL were inducibly expressed in *Mlkl*<sup>-/-</sup> MDFs by  
5 doxycycline, cells were untreated (UT) or treated with TSQ for 6 hrs (please note that this  
6 same control was used in Figure 4A). Cell death was measured by PI staining based on  
7 flow cytometry. Data are plotted as mean ± SEM of three independent experiments.

8 B Cellular fractions from (A) were analysed by Western blot from BN-PAGE or SDS-PAGE  
9 using antibodies as indicated. Representative of three independent experiments.

10 C Cell lysates from (A) were subjected to UBA-pull down and analysed as described above.

11 D N-FLAG MLKL were inducibly expressed in *Mlkl*<sup>-/-</sup> MDFs by doxycycline overnight, and  
12 cells were treated with TSI for indicated time, followed by UBA-pull down.  
13 Representative of three independent experiments.

14 E N-FLAG MLKL were inducibly expressed in *Mlkl*<sup>-/-</sup> MDFs by doxycycline for 16 hrs.  
15 Cells were stimulated ± TSI for 3 hrs after withdrawal of doxycycline. Then TSI medium  
16 was removed and replaced to medium containing inhibitors Bafilomycin A1 (BAF),  
17 PS341 (PS) or left untreated (UT). IDN-6556 was added to all conditions to block  
18 apoptosis. Cells were collected 0, 2, 4, 6 hrs after medium replacement, followed by UBA-  
19 pull down. Representative of three independent experiments.

20

21 **Supplementary Figure 5. N-FLAG MLKL behaves like WT MLKL but does not induce**  
22 **cell death following necroptotic stimulation**

23

24 A WT MLKL and N-FLAG MLKL were inducibly expressed in *Mlkl*<sup>-/-</sup> MDFs by  
25 doxycycline for 12 hrs and cells were treated with the TSI or TSQ necroptotic stimuli. TS  
26 was included to control for responding to apoptosis signalling. Cell death was measured  
27 by PI staining based on flow cytometry. Data are plotted as mean ± SEM of three  
28 independent experiments.

29 B WT MLKL and N-FLAG MLKL were inducibly expressed in *Mlkl*<sup>-/-</sup> MDFs by  
30 doxycycline for 6 hrs, cells were untreated (UT) or treated with TSQ. Cellular fractions  
31 were analysed by Western blot from BN-PAGE or SDS-PAGE using antibodies as  
32 indicated. Representative of three independent experiments.

33

1 **Figure 6. Simultaneous arginine replacement of 4 ubiquitylation sites on the mMLKL**  
2 **4HB domain does not prevent necroptosis-induced ubiquitylation.**

3

4 A Cartoon of the N-terminal region (residues 1-180) of mouse MLKL (PDB accession  
5 4BTF;(Murphy *et al.*, 2013)) showing the four lysine residues identified from MS analysis  
6 as yellow sticks.

7 B WT and 4KR mutant MLKL were inducibly expressed in *Mlkl*<sup>-/-</sup> MDFs by doxycycline for  
8 6 hrs and cells were untreated (UT) or treated with TSI, followed by UBA-pull down.  
9 Representative of three independent experiments.

10

11 **Supplementary Figure 6. Simultaneous arginine replacement of 4 ubiquitylation sites on**  
12 **the mouse MLKL 4HB domain does not prevent necroptosis-induced ubiquitylation.**

13

14 A MS spectra were manually validated to confirm the identification of four Gly-Gly sites on  
15 activated MLKL.

16 B Alignment of mouse and human MLKL N-terminal domain. Positively charged residues  
17 are labelled in blue and negatively charged residues are labelled in pink.

18 C WT and 4KR mutant MLKL were inducibly expressed in *Mlkl*<sup>-/-</sup> MDFs by doxycycline and  
19 cells were treated ± TSI (added simultaneously) for 4 hrs. Sytox Green positive cells were  
20 quantified in real time by IncuCyte S3 live cell imaging. Representative of 3 independent  
21 experiments.

22

23 **Figure 7. MLKL ubiquitylation antagonises necroptosis**

24

25 A Schematic of the MLKL-USP21 and USP21 catalytic dead mutant proteins.

26 B Mouse MLKL-USP21 and MLKL-USP21<sup>C221R</sup> were inducibly expressed in *Mlkl*<sup>-/-</sup> MDFs  
27 by doxycycline (10 ng/mL) for 6 hrs with addition of a necroptotic stimulus (TSI) for  
28 indicated time, followed by UBA-pulldown. Representative of three independent  
29 experiments.

30 C *Mlkl*<sup>-/-</sup> MDFs and *Ripk3*<sup>-/-</sup>*Mlkl*<sup>-/-</sup> MDFs stably transfected with constructs encoding MLKL,  
31 USP21, USP21<sup>C221R</sup>, MLKL-USP21 and MLKL-USP21<sup>C221R</sup> were treated with  
32 doxycycline, TSI or in combination. Propidium iodide positive cells were quantified in  
33 real time by IncuCyte live cell imaging. Representative of three independent experiments.



1 D *MLKL*<sup>-/-</sup> HT29 cells stably transfected with constructs encoding human MLKL-USP21 and  
2 MLKL-USP21<sup>C221R</sup>, were treated with doxycycline, NSA (1 μM), TSI or combinations  
3 thereof (added simultaneously). Sytox Green positive cells were quantified in real time by  
4 live cell imaging. Representative of 6 independent experiments. (A red dashed line is  
5 shown to highlight the delay in death kinetics upon treatment with NSA).

6 E Human MLKL-USP21 and MLKL-USP21<sup>C221R</sup> were inducibly expressed in *MLKL*<sup>-/-</sup>  
7 HT29 cells by doxycycline (10 ng/mL) for 16 hrs and then cells were treated with TSI for  
8 the indicated time course, followed by UBA-pulldown. Representative of three  
9 independent experiments.

10

### 11 **Supplementary Figure 7. MLKL ubiquitylation antagonises necroptosis**

12

13 A Mouse MLKL, human USP21 and mouse MLKL-human USP21 fusions were inducibly  
14 expressed in *Ripk3*<sup>-/-</sup>*Mkl1*<sup>-/-</sup> MDFs following doxycycline addition (20 ng/mL) for 6 hours  
15 ± TSI. Representative of 2 independent experiments.

16 B *MLKL*<sup>-/-</sup> HT29 cells stably transfected with doxycycline inducible constructs encoding  
17 human USP21 and human USP21<sup>C221R</sup> were treated with doxycycline, NSA (1 μM), TSI  
18 or combinations thereof (added simultaneously). Sytox Green positive cells were  
19 quantified in real time by live cell imaging. Representative of 2 independent experiments.

20 C Mouse MLKL-USP21 and MLKL-USP21<sup>C221R</sup> were inducibly expressed in *Mkl1*<sup>-/-</sup> MDFs  
21 by doxycycline (10 ng/mL) for 8 hrs with addition of a necroptotic stimulus (TSI) for 3hrs,  
22 followed by UBA-pulldown and USP21 digestion. Antibody (D6E3G, Cell Signaling  
23 Technology) was used here to detect MLKL phosphorylation. Representative of 2  
24 independent experiments.

25 D *MLKL*<sup>-/-</sup> HT29 cells were stably transfected with indicated doxycycline inducible *MLKL*  
26 alleles (here phosphor-mimic human MLKL mutant T357E/S358E indicated as *MLKL*<sup>TSEE</sup>)  
27 and treated with doxycycline (100 ng/mL) ± TSI (added simultaneously). Representative  
28 of 3 independent experiments.

29

### 30 **References**

31

32 Bertrand MJ, Milutinovic S, Dickson KM, Ho WC, Boudreault A, Durkin J, Gillard JW, Jaquith  
33 JB, Morris SJ, Barker PA (2008) cIAP1 and cIAP2 facilitate cancer cell survival by functioning  
34 as E3 ligases that promote RIP1 ubiquitination. *Mol Cell* 30: 689-700

- 1 Cai Z, Jitkaew S, Zhao J, Chiang HC, Choksi S, Liu J, Ward Y, Wu LG, Liu ZG (2014) Plasma  
2 membrane translocation of trimerized MLKL protein is required for TNF-induced necroptosis.  
3 *Nat Cell Biol* 16: 55-65
- 4 Chen X, Li W, Ren J, Huang D, He WT, Song Y, Yang C, Li W, Zheng X, Chen P *et al* (2014)  
5 Translocation of mixed lineage kinase domain-like protein to plasma membrane leads to  
6 necrotic cell death. *Cell research* 24: 105-121
- 7 Cox J, Neuhauser N, Michalski A, Scheltema RA, Olsen JV, Mann M (2011) Andromeda: a  
8 peptide search engine integrated into the MaxQuant environment. *J Proteome Res* 10:  
9 1794-1805
- 10 Davies KA, Fitzgibbon C, Young SN, Garnish SE, Yeung W, Coursier D, Birkinshaw RW,  
11 Sandow JJ, Lehmann WIL, Liang LY *et al* (2020) Distinct pseudokinase domain conformations  
12 underlie divergent activation mechanisms among vertebrate MLKL orthologues. *Nat*  
13 *Commun* 11: 3060
- 14 Davies KA, Tanzer MC, Griffin MDW, Mok YF, Young SN, Qin R, Petrie EJ, Czabotar PE, Silke J,  
15 Murphy JM (2018) The brace helices of MLKL mediate interdomain communication and  
16 oligomerisation to regulate cell death by necroptosis. *Cell Death Differ* 25: 1567-1580
- 17 Delconte RB, Kolesnik TB, Dagley LF, Rautela J, Shi W, Putz EM, Stannard K, Zhang JG, Teh C,  
18 Firth M *et al* (2016) CIS is a potent checkpoint in NK cell-mediated tumor immunity. *Nat*  
19 *Immunol* 17: 816-824
- 20 Dondelinger Y, Darding M, Bertrand MJ, Walczak H (2016) Poly-ubiquitination in TNFR1-  
21 mediated necroptosis. *Cell Mol Life Sci* 73: 2165-2176
- 22 Dovey CM, Diep J, Clarke BP, Hale AT, McNamara DE, Guo H, Brown NW, Jr., Cao JY, Grace  
23 CR, Gough PJ *et al* (2018) MLKL Requires the Inositol Phosphate Code to Execute  
24 Necroptosis. *Mol Cell* 70: 936-948 e937
- 25 Draber P, Kupka S, Reichert M, Draberova H, Lafont E, de Miguel D, Spilgies L, Surinova S,  
26 Taraborrelli L, Hartwig T *et al* (2015) LUBAC-Recruited CYLD and A20 Regulate Gene  
27 Activation and Cell Death by Exerting Opposing Effects on Linear Ubiquitin in Signaling  
28 Complexes. *Cell Rep* 13: 2258-2272
- 29 Fan W, Guo J, Gao B, Zhang W, Ling L, Xu T, Pan C, Li L, Chen S, Wang H *et al* (2019) Flotillin-  
30 mediated endocytosis and ALIX-syntenin-1-mediated exocytosis protect the cell membrane  
31 from damage caused by necroptosis. *Science signaling* 12
- 32 Gong YN, Guy C, Olauson H, Becker JU, Yang M, Fitzgerald P, Linkermann A, Green DR (2017)  
33 ESCRT-III Acts Downstream of MLKL to Regulate Necroptotic Cell Death and Its  
34 Consequences. *Cell* 169: 286-300 e216
- 35 Haas TL, Emmerich CH, Gerlach B, Schmukle AC, Cordier SM, Rieser E, Feltham R, Vince J,  
36 Warnken U, Wenger T *et al* (2009) Recruitment of the linear ubiquitin chain assembly  
37 complex stabilizes the TNF-R1 signaling complex and is required for TNF-mediated gene  
38 induction. *Mol Cell* 36: 831-844
- 39 Haglund K, Sigismund S, Polo S, Szymkiewicz I, Di Fiore PP, Dikic I (2003) Multiple  
40 monoubiquitination of RTKs is sufficient for their endocytosis and degradation. *Nat Cell Biol*  
41 5: 461-466
- 42 Hancock JF, Cadwallader K, Paterson H, Marshall CJ (1991) A CAAX or a CAAL motif and a  
43 second signal are sufficient for plasma membrane targeting of ras proteins. *EMBO J* 10:  
44 4033-4039
- 45 Hildebrand JM, Kauppi M, Majewski IJ, Liu Z, Cox AJ, Miyake S, Petrie EJ, Silk MA, Li Z, Tanzer  
46 MC *et al* (2020) A missense mutation in the MLKL brace region promotes lethal neonatal  
47 inflammation and hematopoietic dysfunction. *Nat Commun* 11: 3150

- 1 Hildebrand JM, Tanzer MC, Lucet IS, Young SN, Spall SK, Sharma P, Pierotti C, Garnier JM,
- 2 Dobson RC, Webb AI *et al* (2014) Activation of the pseudokinase MLKL unleashes the four-
- 3 helix bundle domain to induce membrane localization and necroptotic cell death. *Proc Natl*
- 4 *Acad Sci U S A* 111: 15072-15077
- 5 Hjerpe R, Aillet F, Lopitz-Otsoa F, Lang V, England P, Rodriguez MS (2009) Efficient
- 6 protection and isolation of ubiquitylated proteins using tandem ubiquitin-binding entities.
- 7 *EMBO Rep* 10: 1250-1258
- 8 Holler N, Zaru R, Micheau O, Thome M, Attinger A, Valitutti S, Bodmer JL, Schneider P, Seed
- 9 B, Tschopp J (2000) Fas triggers an alternative, caspase-8-independent cell death pathway
- 10 using the kinase RIP as effector molecule. *Nat Immunol* 1: 489-495
- 11 Hospenthal MK, Mevissen TET, Komander D (2015) Deubiquitinase-based analysis of
- 12 ubiquitin chain architecture using Ubiquitin Chain Restriction (UbiCRest). *Nat Protoc* 10:
- 13 349-361
- 14 Huang F, Zeng X, Kim W, Balasubramani M, Fortian A, Gygi SP, Yates NA, Sorkin A (2013)
- 15 Lysine 63-linked polyubiquitination is required for EGF receptor degradation. *Proc Natl Acad*
- 16 *Sci U S A* 110: 15722-15727
- 17 Ikeda F, Deribe YL, Skanland SS, Stieglitz B, Grabbe C, Franz-Wachtel M, van Wijk SJ,
- 18 Goswami P, Nagy V, Terzic J *et al* (2011) SHARPIN forms a linear ubiquitin ligase complex
- 19 regulating NF-kappaB activity and apoptosis. *Nature* 471: 637-641
- 20 Jacobsen AV, Lowes KN, Tanzer MC, Lucet IS, Hildebrand JM, Petrie EJ, van Delft MF, Liu Z,
- 21 Conos SA, Zhang JG *et al* (2016) HSP90 activity is required for MLKL oligomerisation and
- 22 membrane translocation and the induction of necroptotic cell death. *Cell Death Dis* 7: e2051
- 23 Kaczmarek A, Vandenabeele P, Krysko DV (2013) Necroptosis: the release of damage-
- 24 associated molecular patterns and its physiological relevance. *Immunity* 38: 209-223
- 25 Kaiser WJ, Sridharan H, Huang C, Mandal P, Upton JW, Gough PJ, Sehon CA, Marquis RW,
- 26 Bertin J, Mocarski ES (2013) Toll-like receptor 3-mediated necrosis via TRIF, RIP3, and MLKL.
- 27 *J Biol Chem* 288: 31268-31279
- 28 Kedzierski L, Tate MD, Hsu AC, Kolesnik TB, Linossi EM, Dagley L, Dong Z, Freeman S, Infusini
- 29 G, Starkey MR *et al* (2017) Suppressor of Cytokine Signaling (SOCS)5 ameliorates influenza
- 30 infection via inhibition of EGFR signaling. *Elife* 6
- 31 Keusekotten K, Elliott PR, Glockner L, Fiil BK, Damgaard RB, Kulathu Y, Wauer T, Hospenthal
- 32 MK, Gyrd-Hansen M, Krappmann D *et al* (2013) OTULIN antagonizes LUBAC signaling by
- 33 specifically hydrolyzing Met1-linked polyubiquitin. *Cell* 153: 1312-1326
- 34 Lacey D, Hickey P, Arhatari BD, O'Reilly LA, Rohrbeck L, Kiriazis H, Du XJ, Bouillet P (2015)
- 35 Spontaneous retrotransposon insertion into TNF 3'UTR causes heart valve disease and
- 36 chronic polyarthritis. *Proc Natl Acad Sci U S A* 112: 9698-9703
- 37 Lawlor KE, Khan N, Mildenhall A, Gerlic M, Croker BA, D'Cruz AA, Hall C, Kaur Spall S,
- 38 Anderton H, Masters SL *et al* (2015) RIPK3 promotes cell death and NLRP3 inflammasome
- 39 activation in the absence of MLKL. *Nat Commun* 6: 6282
- 40 Li D, Xu T, Cao Y, Wang H, Li L, Chen S, Wang X, Shen Z (2015) A cytosolic heat shock protein
- 41 90 and cochaperone CDC37 complex is required for RIP3 activation during necroptosis. *Proc*
- 42 *Natl Acad Sci U S A* 112: 5017-5022
- 43 Liu S, Liu H, Johnston A, Hanna-Addams S, Reynoso E, Xiang Y, Wang Z (2017) MLKL forms
- 44 disulfide bond-dependent amyloid-like polymers to induce necroptosis. *Proc Natl Acad Sci U*
- 45 *S A* 114: E7450-E7459
- 46 Liu Z, Silke J, Hildebrand JM (2018) Methods for Studying TNF-Mediated Necroptosis in
- 47 Cultured Cells. *Methods Mol Biol* 1857: 53-61

- 1 Menon MB, Gaestel M (2018) MK2-TNF-Signaling Comes Full Circle. *Trends Biochem Sci* 43:
- 2 170-179
- 3 Morrow ME, Morgan MT, Clerici M, Growkova K, Yan M, Komander D, Sixma TK, Simicek M,
- 4 Wolberger C (2018) Active site alanine mutations convert deubiquitinases into high-affinity
- 5 ubiquitin-binding proteins. *EMBO Rep* 19
- 6 Mosesson Y, Yarden Y (2006) Monoubiquitylation: a recurrent theme in membrane protein
- 7 transport. *Isr Med Assoc J* 8: 233-237
- 8 Moujalled DM, Cook WD, Murphy JM, Vaux DL (2014) Necroptosis induced by RIPK3
- 9 requires MLKL but not Drp1. *Cell Death Dis* 5: e1086
- 10 Murai S, Yamaguchi Y, Shirasaki Y, Yamagishi M, Shindo R, Hildebrand JM, Miura R,
- 11 Nakabayashi O, Totsuka M, Tomida T *et al* (2018) A FRET biosensor for necroptosis uncovers
- 12 two different modes of the release of DAMPs. *Nat Commun* 9: 4457
- 13 Murphy JM, Czabotar PE, Hildebrand JM, Lucet IS, Zhang JG, Alvarez-Diaz S, Lewis R, Lalaoui
- 14 N, Metcalf D, Webb AI *et al* (2013) The pseudokinase MLKL mediates necroptosis via a
- 15 molecular switch mechanism. *Immunity* 39: 443-453
- 16 Oh E, Akopian D, Rape M (2018) Principles of Ubiquitin-Dependent Signaling. *Annu Rev Cell*
- 17 *Dev Biol* 34: 137-162
- 18 Onizawa M, Oshima S, Schulze-Topphoff U, Oses-Prieto JA, Lu T, Tavares R, Prodhomme T,
- 19 Duong B, Whang MI, Advincula R *et al* (2015) The ubiquitin-modifying enzyme A20 restricts
- 20 ubiquitination of the kinase RIPK3 and protects cells from necroptosis. *Nat Immunol* 16:
- 21 618-627
- 22 Orozco S, Yatim N, Werner MR, Tran H, Gunja SY, Tait SW, Albert ML, Green DR, Oberst A
- 23 (2014) RIPK1 both positively and negatively regulates RIPK3 oligomerization and necroptosis.
- 24 *Cell Death Differ* 21: 1511-1521
- 25 Perez-Riverol Y, Csordas A, Bai J, Bernal-Llinares M, Hewapathirana S, Kundu DJ, Inuganti A,
- 26 Griss J, Mayer G, Eisenacher M *et al* (2019) The PRIDE database and related tools and
- 27 resources in 2019: improving support for quantification data. *Nucleic Acids Res* 47: D442-
- 28 D450
- 29 Petersen SL, Chen TT, Lawrence DA, Marsters SA, Gonzalez F, Ashkenazi A (2015) TRAF2 is a
- 30 biologically important necroptosis suppressor. *Cell Death Differ* 22: 1846-1857
- 31 Petrie EJ, Birkinshaw RW, Koide A, Denbaum E, Hildebrand JM, Garnish SE, Davies KA,
- 32 Sandow JJ, Samson AL, Gavin X *et al* (2020) Identification of MLKL membrane translocation
- 33 as a checkpoint in necroptotic cell death using Monobodies. *Proc Natl Acad Sci U S A* 117:
- 34 8468-8475
- 35 Petrie EJ, Czabotar PE, Murphy JM (2019a) The Structural Basis of Necroptotic Cell Death
- 36 Signaling. *Trends Biochem Sci* 44: 53-63
- 37 Petrie EJ, Sandow JJ, Jacobsen AV, Smith BJ, Griffin MDW, Lucet IS, Dai W, Young SN, Tanzer
- 38 MC, Wardak A *et al* (2018) Conformational switching of the pseudokinase domain promotes
- 39 human MLKL tetramerization and cell death by necroptosis. *Nat Commun* 9: 2422
- 40 Petrie EJ, Sandow JJ, Lehmann WIL, Liang LY, Coursier D, Young SN, Kersten WJA, Fitzgibbon
- 41 C, Samson AL, Jacobsen AV *et al* (2019b) Viral MLKL Homologs Subvert Necroptotic Cell
- 42 Death by Sequestering Cellular RIPK3. *Cell Rep* 28: 3309-3319 e3305
- 43 Petroski MD, Deshaies RJ (2003) Context of multiubiquitin chain attachment influences the
- 44 rate of Sic1 degradation. *Mol Cell* 11: 1435-1444
- 45 Samson AL, Zhang Y, Geoghegan ND, Gavin XJ, Davies KA, Mlodzianoski MJ, Whitehead LW,
- 46 Frank D, Garnish SE, Fitzgibbon C *et al* (2020) MLKL trafficking and accumulation at the
- 47 plasma membrane control the kinetics and threshold for necroptosis. *Nat Commun* 11: 3151

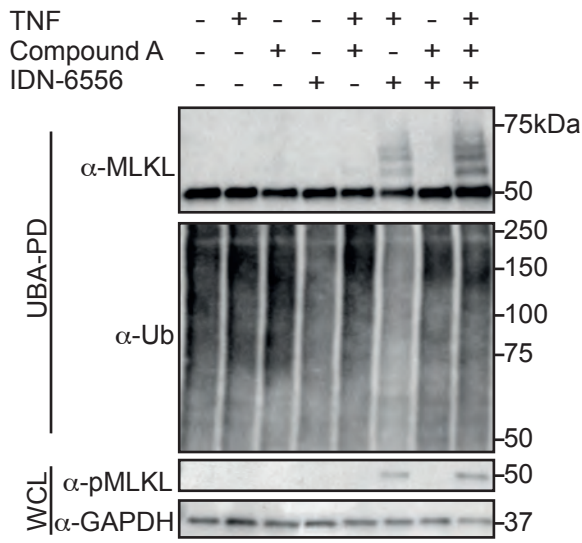
- 1 Sapmaz A, Berlin I, Bos E, Wijdeven RH, Janssen H, Konietzny R, Akkermans JJ, Erson-Bensan
- 2 AE, Koning RI, Kessler BM *et al* (2019) USP32 regulates late endosomal transport and
- 3 recycling through deubiquitylation of Rab7. *Nat Commun* 10: 1454
- 4 Schagger H, von Jagow G (1991) Blue native electrophoresis for isolation of membrane
- 5 protein complexes in enzymatically active form. *Anal Biochem* 199: 223-231
- 6 Segawa K, Nagata S (2015) An Apoptotic 'Eat Me' Signal: Phosphatidylserine Exposure.
- 7 *Trends Cell Biol* 25: 639-650
- 8 Stafford CA, Lawlor KE, Heim VJ, Bankovacki A, Bernardini JP, Silke J, Nachbur U (2018) IAPs
- 9 Regulate Distinct Innate Immune Pathways to Co-ordinate the Response to Bacterial
- 10 Peptidoglycans. *Cell Rep* 22: 1496-1508
- 11 Sun X, Yin J, Starovasnik MA, Fairbrother WJ, Dixit VM (2002) Identification of a novel
- 12 homotypic interaction motif required for the phosphorylation of receptor-interacting
- 13 protein (RIP) by RIP3. *J Biol Chem* 277: 9505-9511
- 14 Swatek KN, Komander D (2016) Ubiquitin modifications. *Cell Res* 26: 399-422
- 15 Tanzer MC, Matti I, Hildebrand JM, Young SN, Wardak A, Tripaydonis A, Petrie EJ, Mildenhall
- 16 AL, Vaux DL, Vince JE *et al* (2016) Evolutionary divergence of the necroptosis effector MLKL.
- 17 *Cell Death Differ* 23: 1185-1197
- 18 Tanzer MC, Tripaydonis A, Webb AI, Young SN, Varghese LN, Hall C, Alexander WS,
- 19 Hildebrand JM, Silke J, Murphy JM (2015) Necroptosis signalling is tuned by phosphorylation
- 20 of MLKL residues outside the pseudokinase domain activation loop. *Biochem J* 471: 255-265
- 21 Tokunaga F, Sakata S, Saeki Y, Satomi Y, Kirisako T, Kamei K, Nakagawa T, Kato M, Murata S,
- 22 Yamaoka S *et al* (2009) Involvement of linear polyubiquitylation of NEMO in NF-kappaB
- 23 activation. *Nat Cell Biol* 11: 123-132
- 24 Vanden Berghe T, Kaiser WJ, Bertrand MJ, Vandenabeele P (2015) Molecular crosstalk
- 25 between apoptosis, necroptosis, and survival signaling. *Mol Cell Oncol* 2: e975093
- 26 Vandenabeele P, Riquet F, Cappe B (2017) Necroptosis: (Last) Message in a Bubble.
- 27 *Immunity* 47: 1-3
- 28 Wang H, Sun L, Su L, Rizo J, Liu L, Wang LF, Wang FS, Wang X (2014) Mixed lineage kinase
- 29 domain-like protein MLKL causes necrotic membrane disruption upon phosphorylation by
- 30 RIP3. *Mol Cell* 54: 133-146
- 31 Wang Z, Jiang H, Chen S, Du F, Wang X (2012) The mitochondrial phosphatase PGAM5
- 32 functions at the convergence point of multiple necrotic death pathways. *Cell* 148: 228-243
- 33 Weber K, Roelandt R, Bruggeman I, Estornes Y, Vandenabeele P (2018) Nuclear RIPK3 and
- 34 MLKL contribute to cytosolic necrosome formation and necroptosis. *Commun Biol* 1: 6
- 35 Wilkinson KD, Tashayev VL, O'Connor LB, Larsen CN, Kasperk E, Pickart CM (1995)
- 36 Metabolism of the polyubiquitin degradation signal: structure, mechanism, and role of
- 37 isopeptidase T. *Biochemistry* 34: 14535-14546
- 38 Wisniewski JR, Zougman A, Nagaraj N, Mann M (2009) Universal sample preparation
- 39 method for proteome analysis. *Nat Methods* 6: 359-362
- 40 Wright LP, Philips MR (2006) Thematic review series: lipid posttranslational modifications.
- 41 CAAX modification and membrane targeting of Ras. *J Lipid Res* 47: 883-891
- 42 Wu G, Xu G, Schulman BA, Jeffrey PD, Harper JW, Pavletich NP (2003) Structure of a beta-
- 43 TrCP1-Skp1-beta-catenin complex: destruction motif binding and lysine specificity of the
- 44 SCF(beta-TrCP1) ubiquitin ligase. *Mol Cell* 11: 1445-1456
- 45 Wu XN, Yang ZH, Wang XK, Zhang Y, Wan H, Song Y, Chen X, Shao J, Han J (2014) Distinct
- 46 roles of RIP1-RIP3 hetero- and RIP3-RIP3 homo-interaction in mediating necroptosis. *Cell*
- 47 *Death Differ* 21: 1709-1720

- 1 Ye Y, Akutsu M, Reyes-Turcu F, Enchev RI, Wilkinson KD, Komander D (2011) Polyubiquitin
- 2 binding and cross-reactivity in the USP domain deubiquitinase USP21. *EMBO Rep* 12: 350-
- 3 357
- 4 Ye Y, Blaser G, Horrocks MH, Ruedas-Rama MJ, Ibrahim S, Zhukov AA, Orte A, Klenerman D,
- 5 Jackson SE, Komander D (2012) Ubiquitin chain conformation regulates recognition and
- 6 activity of interacting proteins. *Nature* 492: 266-270
- 7 Yoon S, Bogdanov K, Kovalenko A, Wallach D (2016) Necroptosis is preceded by nuclear
- 8 translocation of the signaling proteins that induce it. *Cell Death Differ* 23: 253-260
- 9 Yoon S, Kovalenko A, Bogdanov K, Wallach D (2017) MLKL, the Protein that Mediates
- 10 Necroptosis, Also Regulates Endosomal Trafficking and Extracellular Vesicle Generation.
- 11 *Immunity* 47: 51-65 e57
- 12 Zargarian S, Shlomovitz I, Erlich Z, Hourizadeh A, Ofir-Birin Y, Croker BA, Regev-Rudzki N,
- 13 Edry-Botzer L, Gerlic M (2017) Phosphatidylserine externalization, "necroptotic bodies"
- 14 release, and phagocytosis during necroptosis. *PLoS Biol* 15: e2002711
- 15
- 16
- 17 **END**

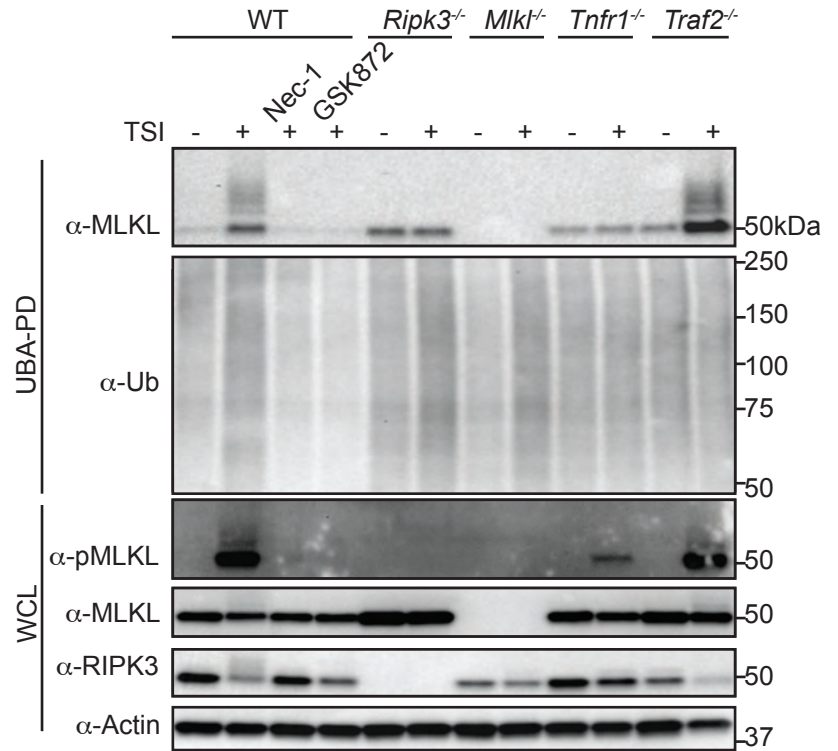
# Figure 1. MLKL undergoes ubiquitylation during necroptosis

bioRxiv preprint doi: <https://doi.org/10.1101/2021.05.01.442209>; this version posted May 1, 2021. The copyright holder for this preprint (which was not certified by peer review) is the author/funder. All rights reserved. No reuse allowed without permission.

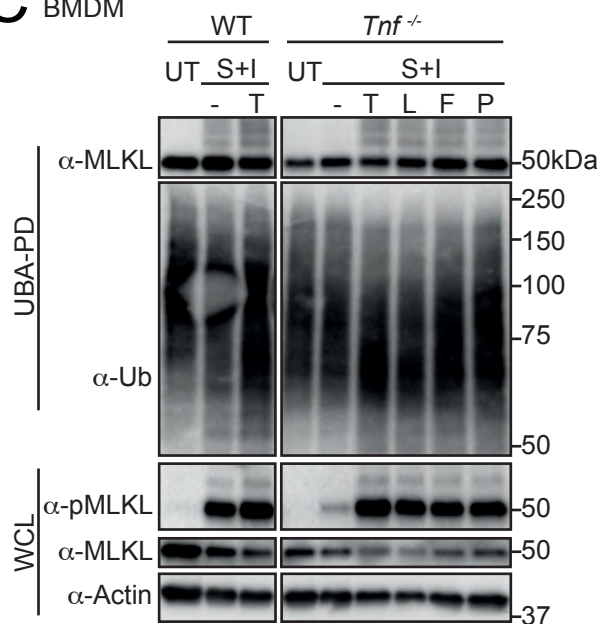
## A WT MDF



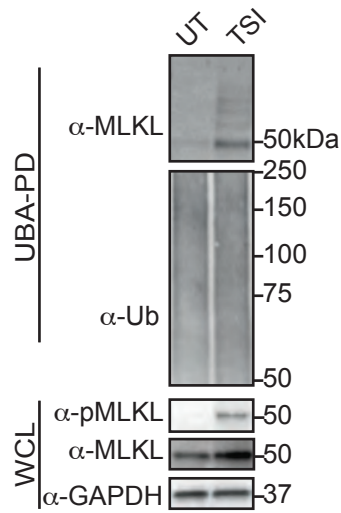
## B MDF



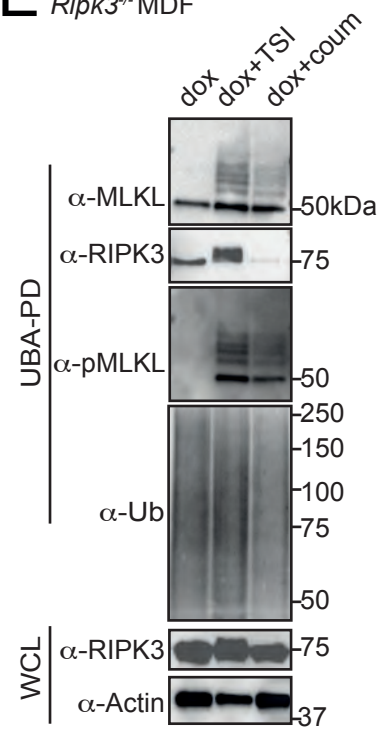
## C BMDM



## D WT HT29



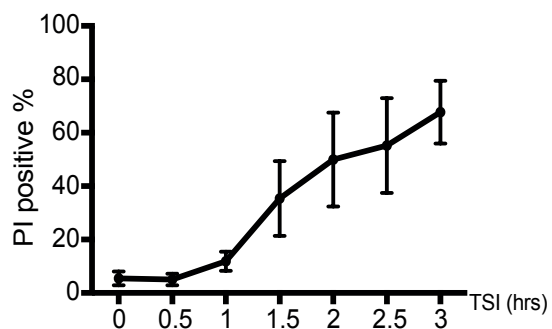
## E *Ripk3*<sup>-/-</sup> MDF



### Supplementary Figure 1. Cell death time course of MDFs and HT29 cells following necroptotic stimulation

bioRxiv preprint doi: <https://doi.org/10.1101/2021.05.01.442209>; this version posted May 1, 2021. The copyright holder for this preprint (which was not certified by peer review) is the author/funder. All rights reserved. No reuse allowed without permission.

**A** WT MDF



**B** WT HT29

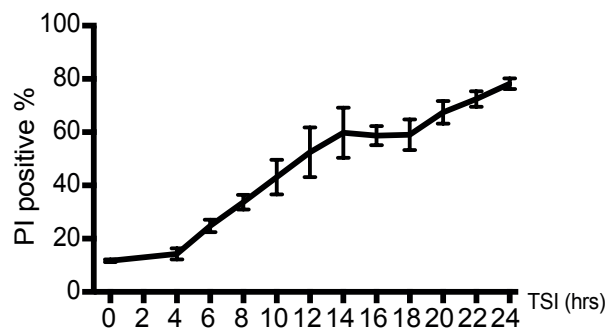




## Figure 2. MLKL is mono-ubiquitylated at multiple sites

bioRxiv preprint doi: <https://doi.org/10.1101/2021.05.01.442209>; this version posted May 1, 2021. The copyright holder for this preprint (which was not certified by peer review) is the author/funder. All rights reserved. No reuse allowed without permission.

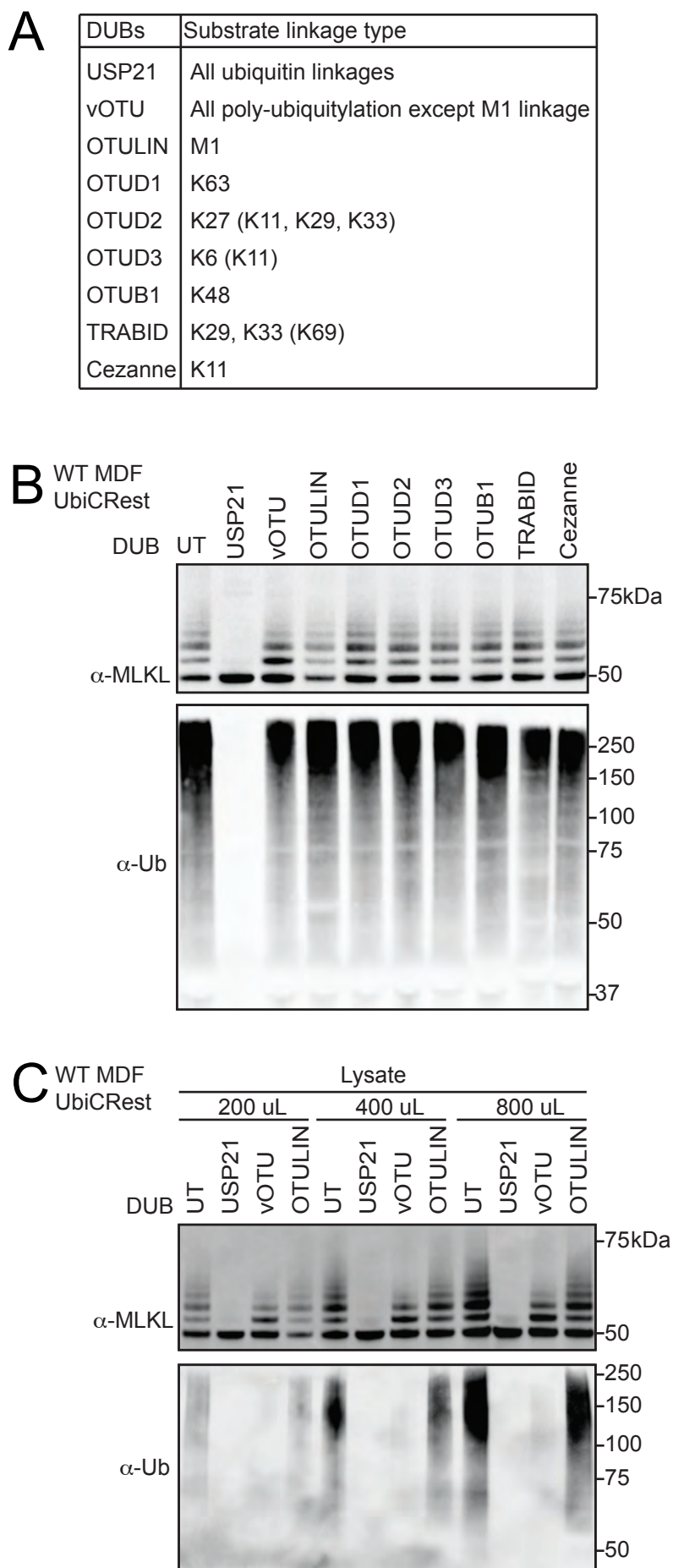
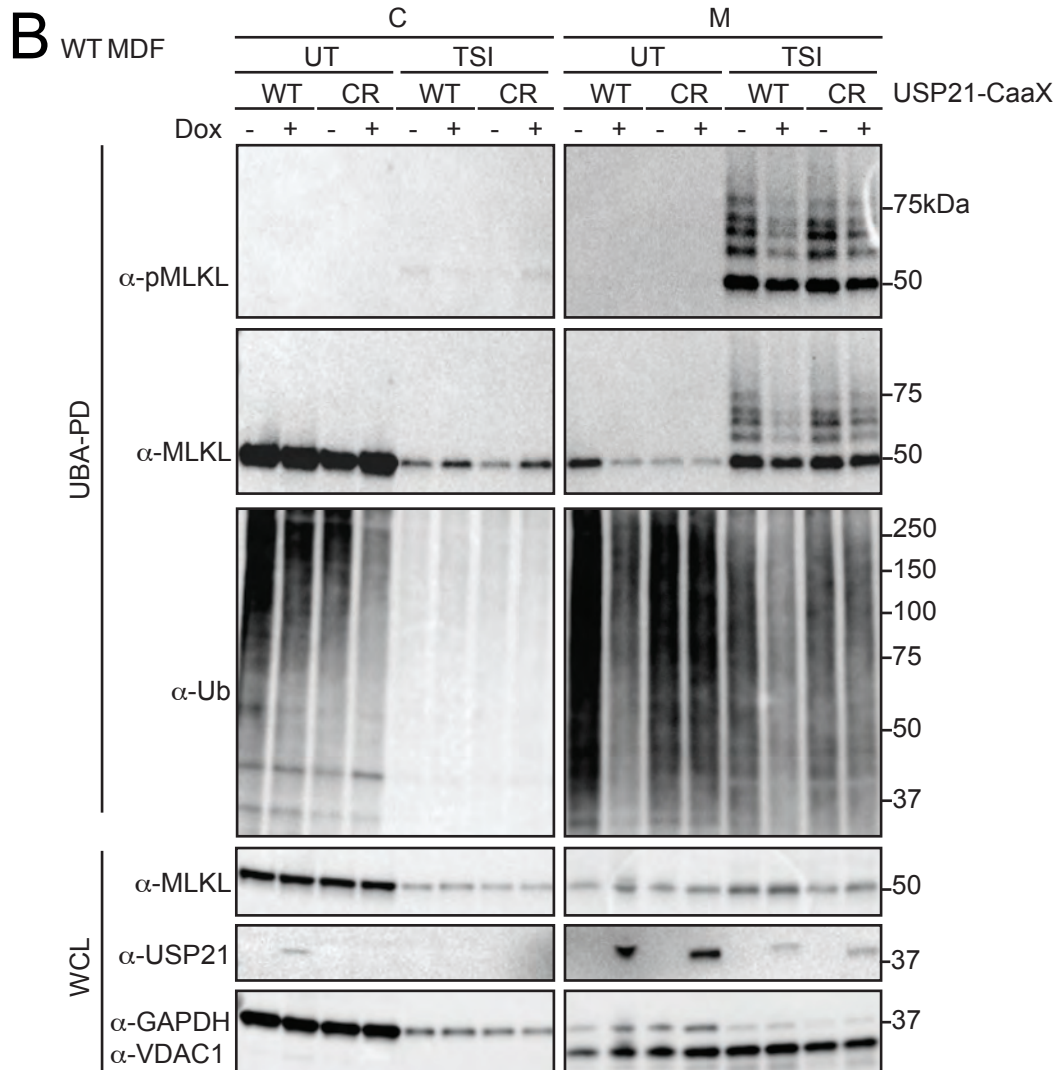
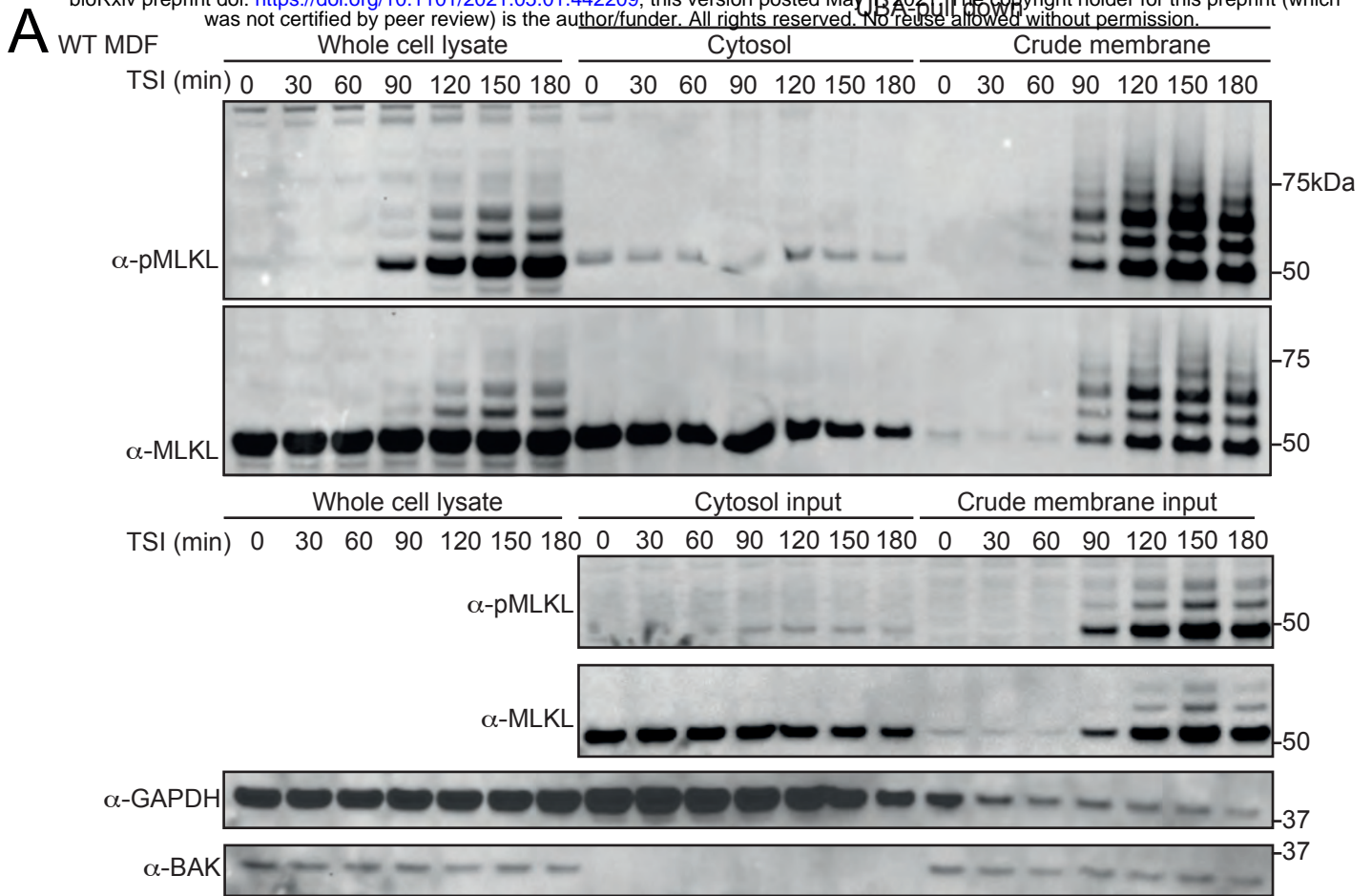


**Figure 3. MLKL ubiquitylation accumulates in crude membranes and can be digested by USP21 located on biological membranes.**

bioRxiv preprint doi: <https://doi.org/10.1101/2021.05.01.442209>; this version posted May 1, 2021. The copyright holder for this preprint (which was not certified by peer review) is the author/funder. All rights reserved. No reuse allowed without permission.



### Supplementary Figure 3. USP21-CaaX expression does not alter the kinetics of TNF induced apoptosis or necroptosis in MDFs

bioRxiv preprint doi: <https://doi.org/10.1101/2021.05.01.442209>; this version posted May 1, 2021. The copyright holder for this preprint (which was not certified by peer review) is the author/funder. All rights reserved. No reuse allowed without permission.

WT MDF

A

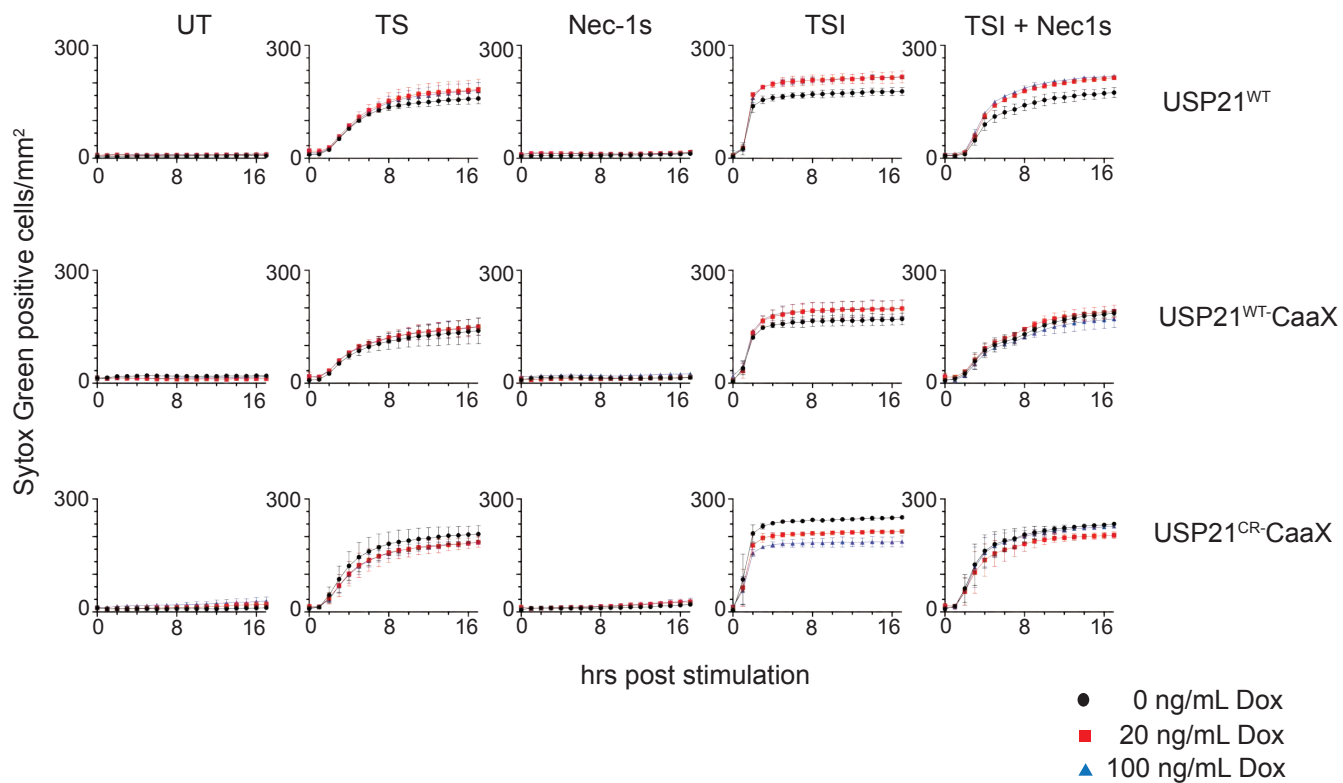
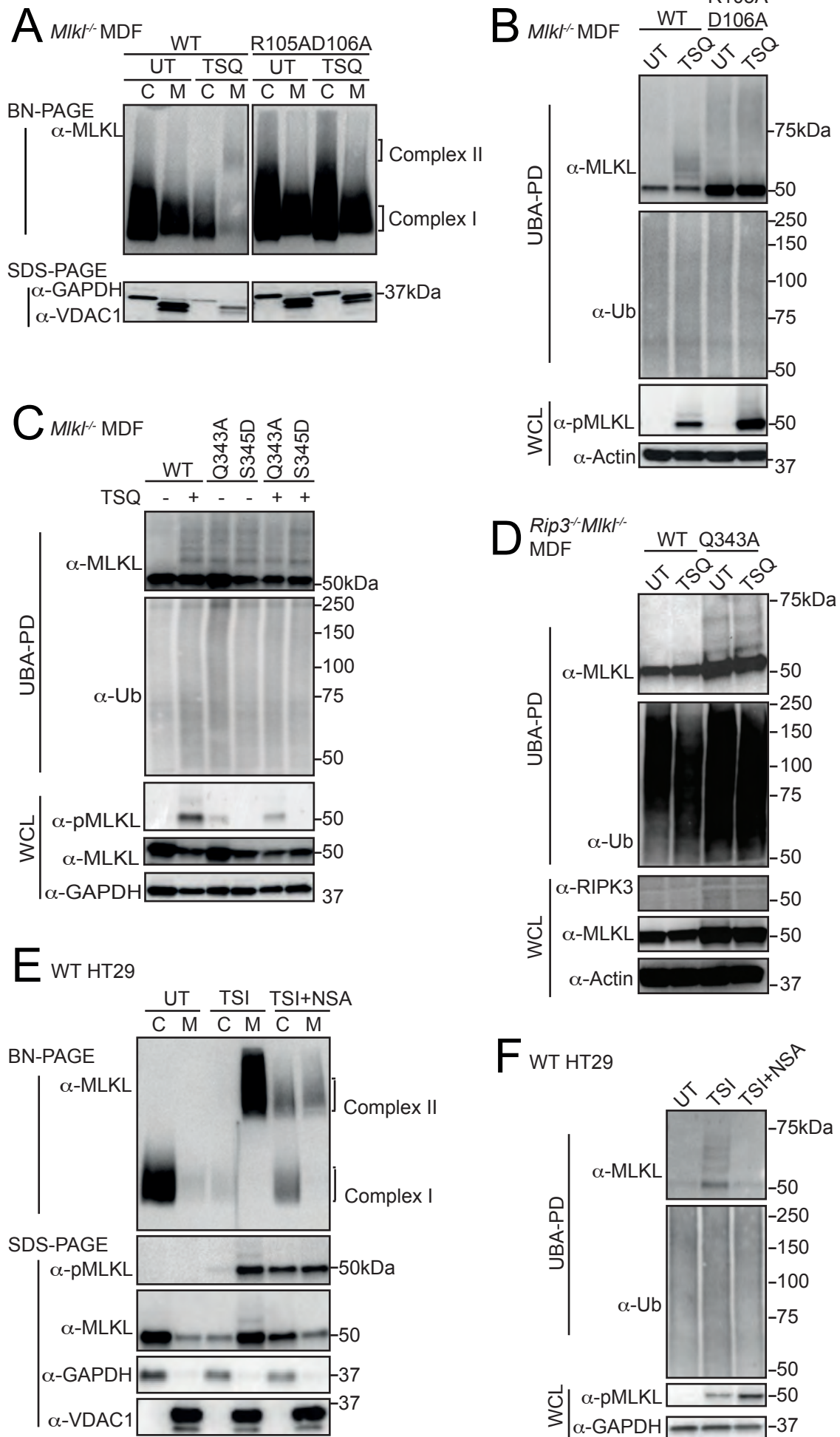


**Figure 4. MLKL oligomerization drives its necroptosis specific ubiquitylation**

bioRxiv preprint doi: <https://doi.org/10.1101/2021.05.01.442209>; this version posted May 1, 2021. The copyright holder for this preprint (which was not certified by peer review) is the author/funder. All rights reserved. No reuse allowed without permission.



## Supplementary Figure 4. MLKL oligomerization drives its necroptosis specific ubiquitylation

bioRxiv preprint doi: <https://doi.org/10.1101/2021.05.01.442209>; this version posted May 1, 2021. The copyright holder for this preprint (which was not certified by peer review) is the author/funder. All rights reserved. No reuse allowed without permission.

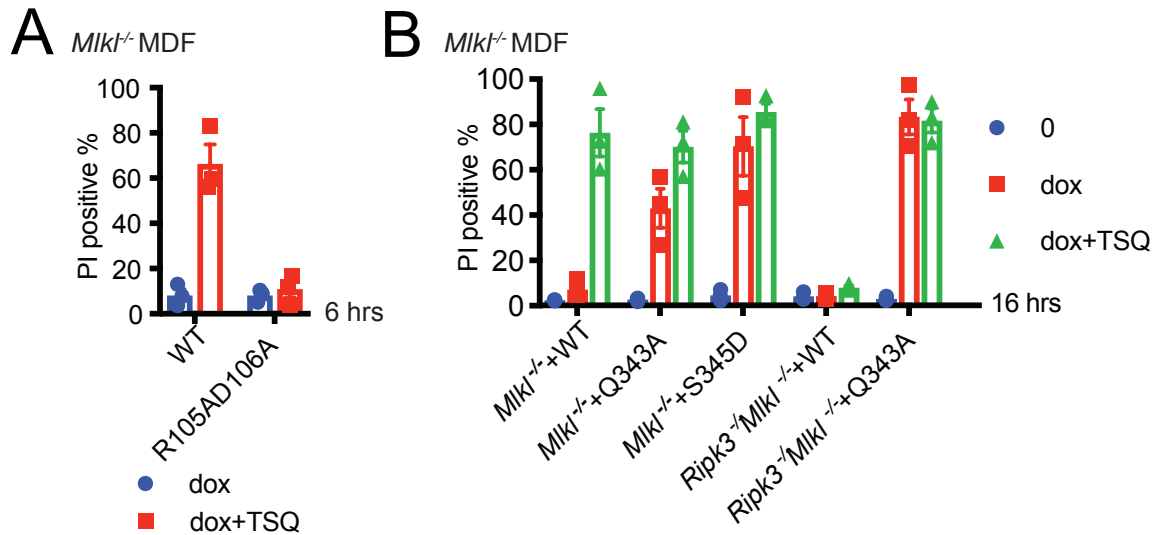
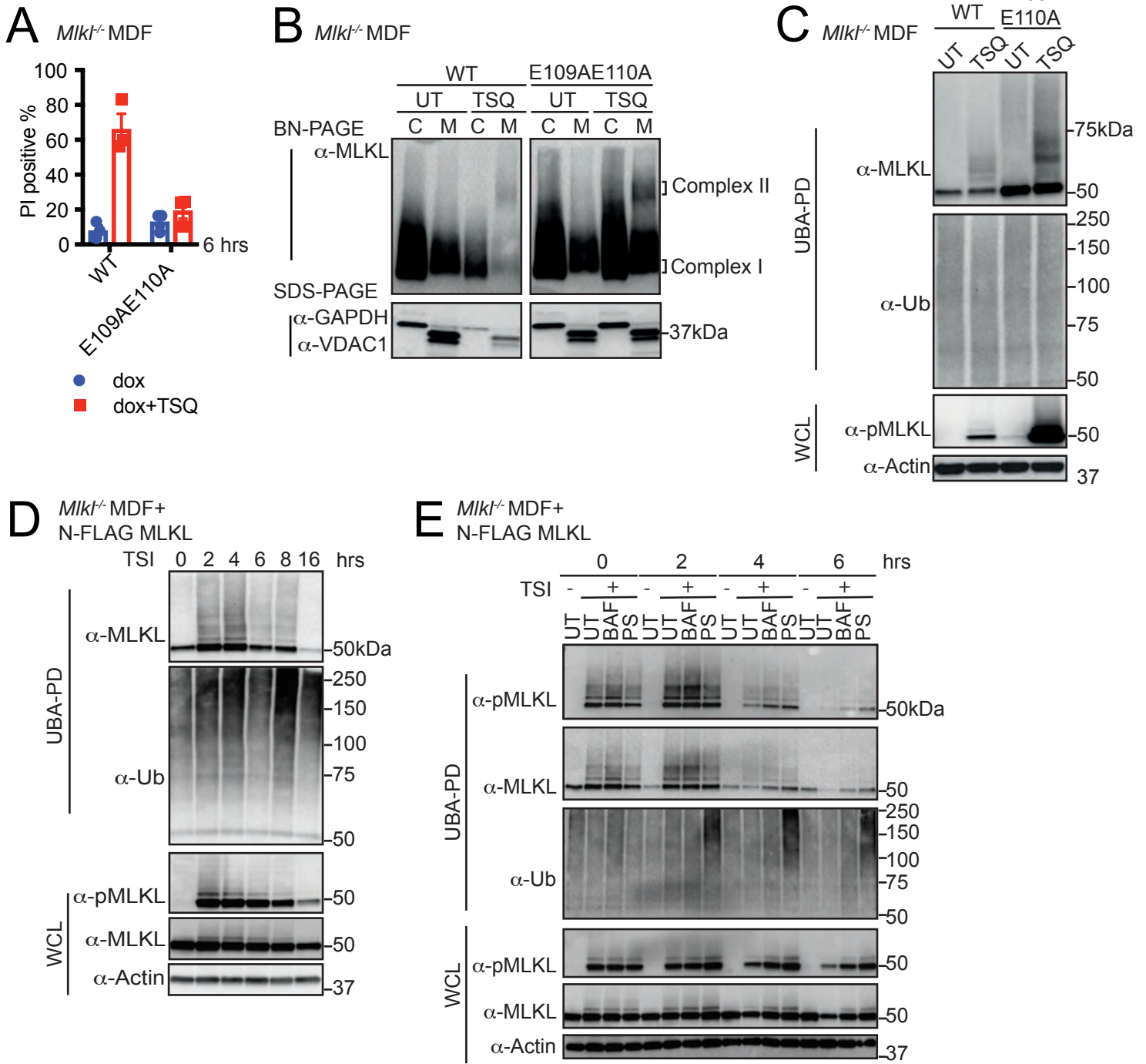


**Figure 5. MLKL ubiquitylation does not lead to cell death, but correlates with the turnover of activated MLKL**

bioRxiv preprint doi: <https://doi.org/10.1101/2021.05.01.442209>; this version posted May 1, 2021. The copyright holder for this preprint (which was not certified by peer review) is the author/funder. All rights reserved. No reuse allowed without permission.



**Supplementary Figure 5. N-FLAG MLKL behaves like WT MLKL but does not induce cell death following necroptotic stimulation**

bioRxiv preprint doi: <https://doi.org/10.1101/2021.05.01.442209>; this version posted May 1, 2021. The copyright holder for this preprint (which was not certified by peer review) is the author/funder. All rights reserved. No reuse allowed without permission.

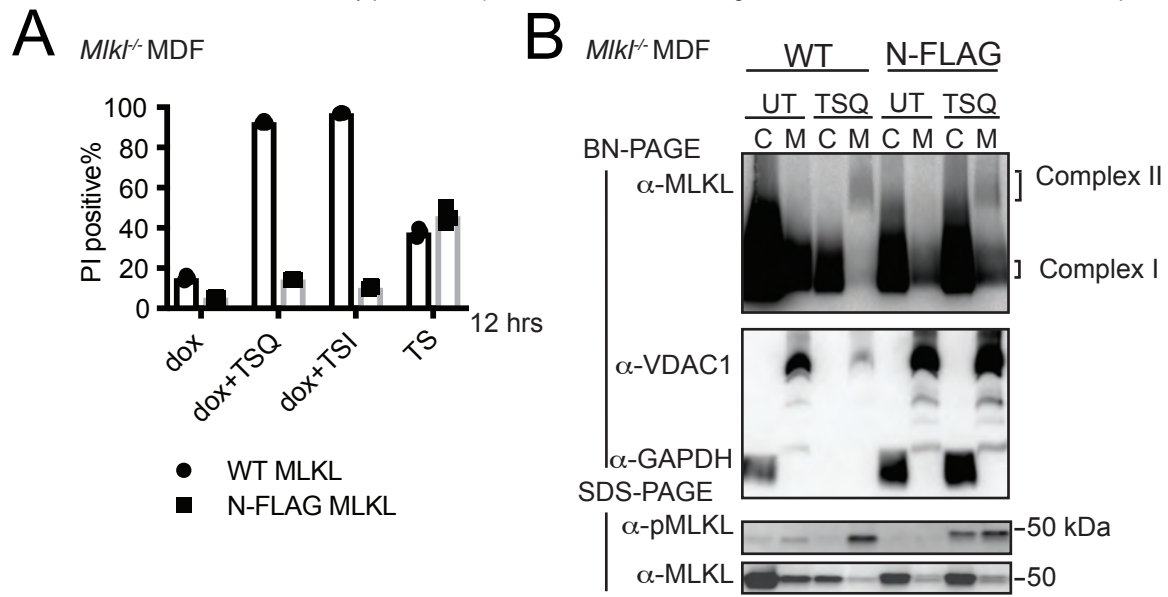
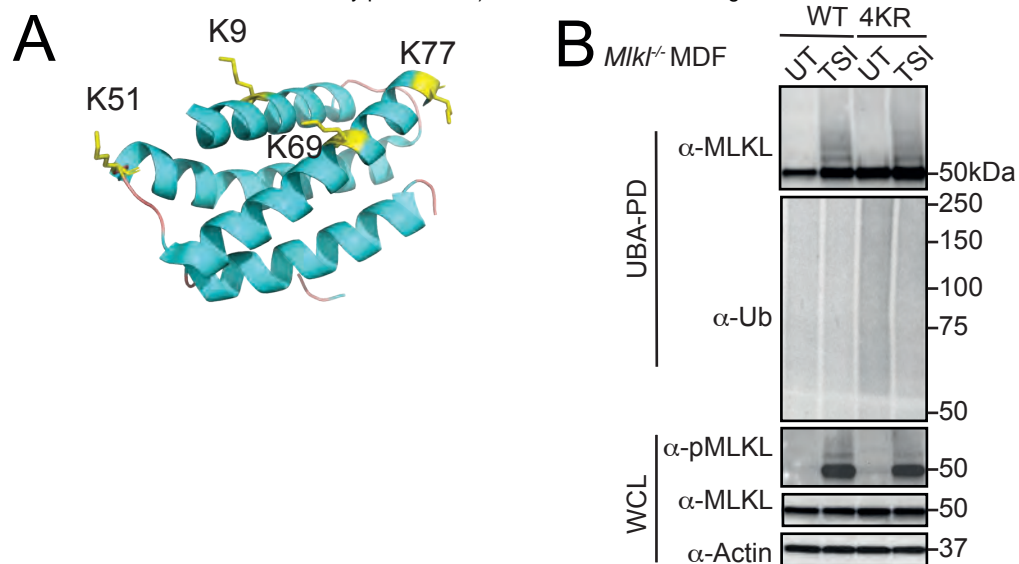




**Figure 6. Simultaneous arginine replacement of 4 ubiquitylation sites on the mMLKL 4HB domain does not prevent necroptosis-induced ubiquitylation**

bioRxiv preprint doi: <https://doi.org/10.1101/2021.05.01.442209>; this version posted May 1, 2021. The copyright holder for this preprint (which was not certified by peer review) is the author/funder. All rights reserved. No reuse allowed without permission.





**Supplementary Figure 6. Simultaneous arginine replacement of 4 ubiquitylation sites on the mouse MLKL 4HB domain does not prevent necroptosis-induced ubiquitylation**

bioRxiv preprint doi: <https://doi.org/10.1101/2021.05.01.442208>; this version posted May 1, 2021. The copyright holder for this preprint (which was not certified by peer review) is the author/funder. All rights reserved. No reuse allowed without permission.

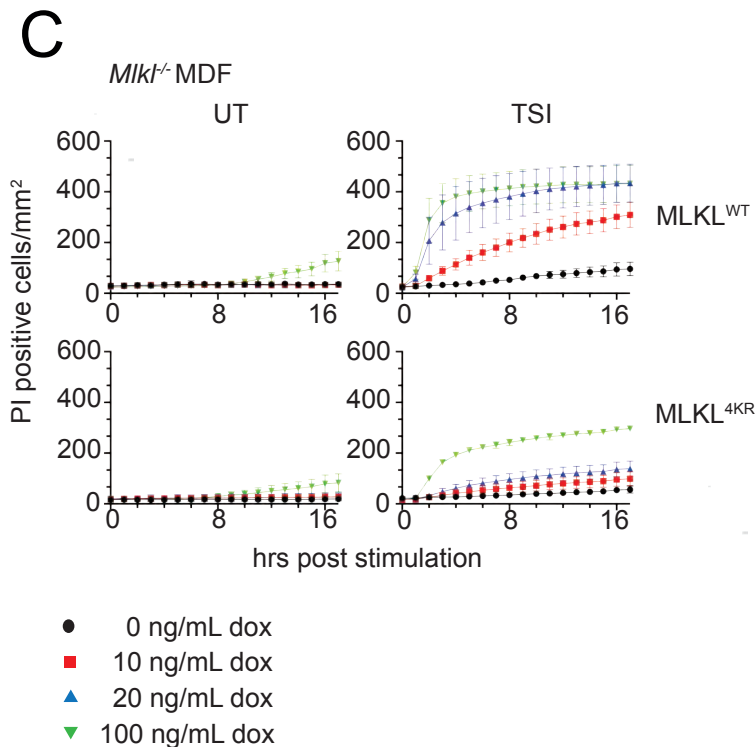
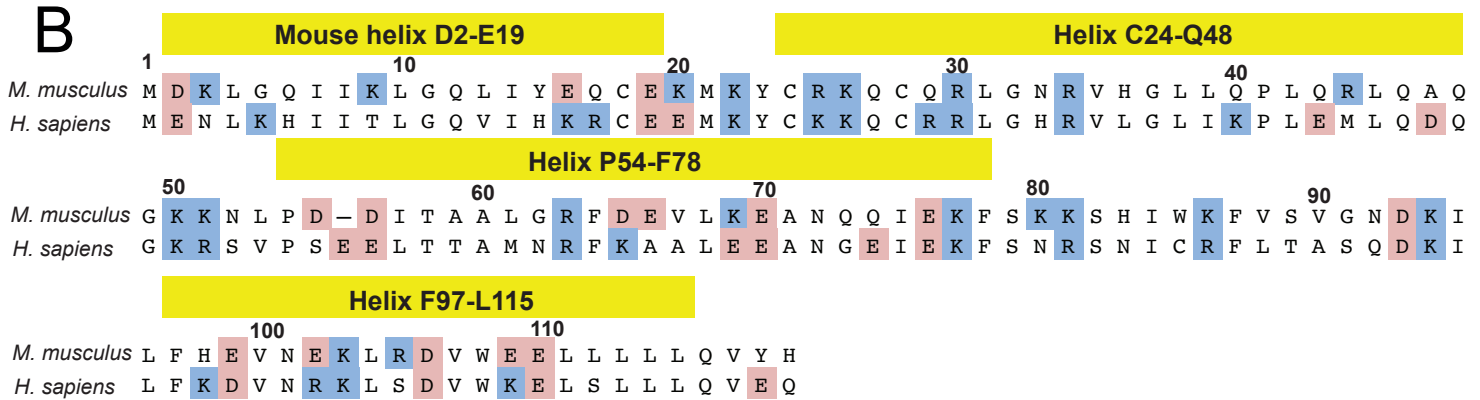
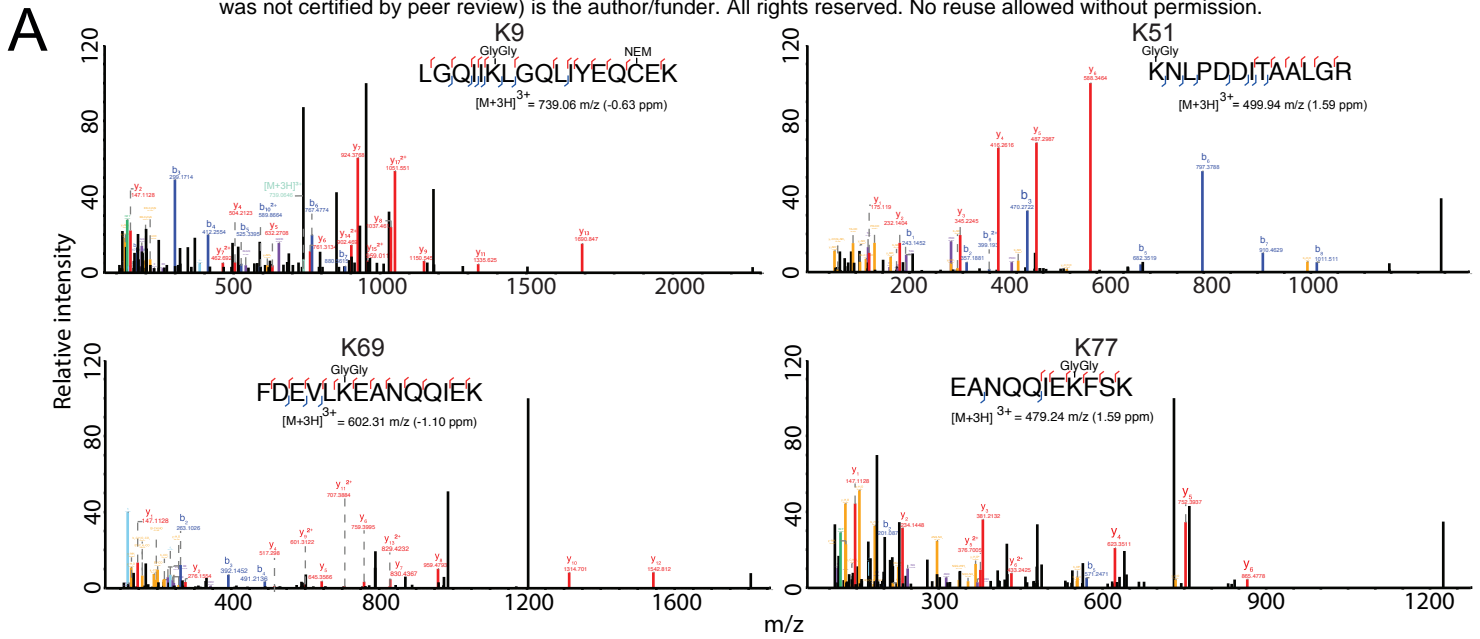
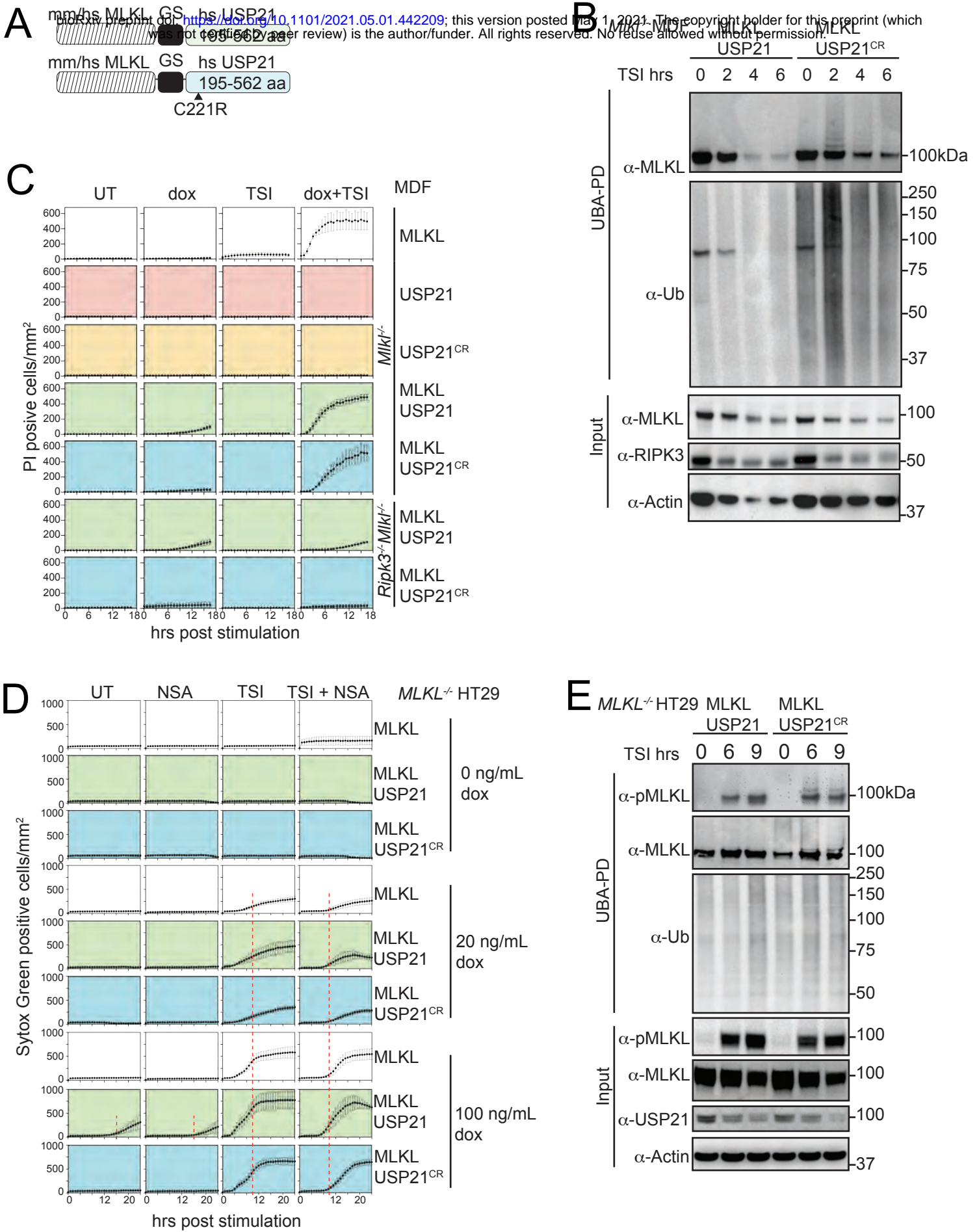


**Figure 7. MLKL ubiquitylation antagonises necroptosis**



**Supplementary Figure 7. MLKL ubiquitylation antagonises necroptosis**

